A role for the metalloprotease invadolysin in insulin signaling and adipogenesis

Ching-Wen Chang[a,b], Kanishk Abhinav[a], Francesca Di Cara[c], Ioanna Panagakou, Sharron Vass[d] and Margarete M.S. Heck*

A role for the metalloprotease invadolysin in insulin signaling and adipogenesis

DOI 10.1515/hsz-2016-0226
Received June 8, 2016; accepted September 4, 2016

Abstract: Invadolysin is a novel metalloprotease conserved amongst metazoans that is essential for life in *Drosophila*. We previously showed that invadolysin was essential for the cell cycle and cell migration, linking to metabolism through a role in lipid storage and interaction with mitochondrial proteins. In this study we demonstrate that *invadolysin* mutants exhibit increased autophagy and decreased glycogen storage – suggestive of a role for invadolysin in insulin signaling in *Drosophila*. Consistent with this, effectors of insulin signaling were decreased in *invadolysin* mutants. In addition, we discovered that invadolysin was deposited on newly synthesized lipid droplets in a PKC-dependent manner. We examined two *in vitro* models of adipogenesis for the expression and localization of invadolysin. The level of invadolysin increased during both murine 3T3-L1 and human Simpson-Golabi-Behmel syndrome (SGBS), adipogenesis. Invadolysin displayed a dynamic localization to lipid droplets over the course of adipogenesis, which may be due to the differential expression of distinct invadolysin variants. Pharmacological inhibition of adipogenesis abrogated the increase in invadolysin. In summary, our results on *in vivo* and *in vitro* systems highlight an important role for invadolysin in insulin signaling and adipogenesis.

Keywords: adipogenesis; insulin signaling; lipid droplets; metalloprotease.

[a]**Ching-Wen Chang and Kanishk Abhinav:** These authors contributed equally to this work.
[b]Present address: Institute of Biomedical Sciences, Academia Sinica, Taipei 11529, Taiwan.
[c]Present address: Department of Cell Biology, Faculty of Medicine, University of Alberta, Edmonton T6G 2H7, Canada.
[d]Present address: Edinburgh Napier University, Sighthill Court, Edinburgh EH11 4BN, UK.
***Corresponding author: Margarete M.S. Heck,** University of Edinburgh, Queen's Medical Research Institute, University/BHF Center for Cardiovascular Science, 47 Little France Crescent, Edinburgh EH16 4TJ, UK, e-mail: margarete.heck@ed.ac.uk
Ching-Wen Chang, Kanishk Abhinav, Francesca Di Cara, Ioanna Panagakou and Sharron Vass: University of Edinburgh, Queen's Medical Research Institute, University/BHF Center for Cardiovascular Science, 47 Little France Crescent, Edinburgh EH16 4TJ, UK

Introduction

Proteases – whether aspartic, cysteine, glutamic, asparagine, serine/threonine or metallo – play diverse and crucial intracellular and extracellular roles (Rawlings and Barrett, 1999; Gomis-Ruth, 2003). Invadolysin is a member of the M8 family of metzincin metalloproteases strikingly represented in most metazoans by a single gene, in contrast to the multi-gene MMP or ADAM families. *Drosophila invadolysin* mutant larvae die during the late larval stages with aberrantly condensed chromosomes and monopolar spindles in dividing larval neuroblasts (McHugh et al., 2004). The *invadolysin* mutant animals have increased levels of lamin and otefin nuclear envelope proteins, and mono-ubiquitinated histone H2B (McHugh et al., 2004; Rao et al., 2015). A role for invadolysin in cell migration is evident in both *Drosophila* mutant larvae and zebrafish embryos depleted of invadolysin by morpholino interference (McHugh et al., 2004; Vass and Heck, 2013). Invadolysin localizes to lipid droplets in cultured cell lines (Cobbe et al., 2009) and plays a role in metabolism through interaction with ATP synthase subunits (Di Cara et al., 2013). That *invadolysin* mutant larvae have a decreased lipid:protein ratio suggests that the enzyme may play a functional role in lipid accumulation (Cobbe et al., 2009). Storage of proteins, including core histones, in lipid droplets presents an intriguing link between the localization of invadolysin to lipid droplets and the abnormal chromosome morphology in *invadolysin* mutants (Cermelli et al., 2006; Li et al., 2012; Welte, 2015).

Lipid droplets were initially considered to be relatively inert organelles whose sole function was to store neutral lipids as triglycerides and cholesterol esters (Goldberg et al., 2009; Walther and Farese, 2012; Welte, 2015). Several studies on lipid droplets have shown these structures to be dynamic and involved in many vital activities (Welte, 2015), including the regulation of lipid homeostasis (Smirnova et al., 2006; Naslavsky et al., 2007) but also in less intuitively obvious processes such as protein storage (Cermelli et al., 2006). Morphological changes in lipid droplets observed in conditions such as cancer (Accioly et al., 2008), Parkinson's disease (Scherzer et al., 2003), and longevity regulation (Goldberg et al., 2009) link lipid droplets to vertebrate physiology and disease.

Lipid droplet proteins are dynamically regulated during adipogenesis. The size and number of lipid droplets increases and the levels of lipid droplet associated proteins including adipose triglyceride lipase (ATGL), CGI-58, perilipin and adipose differentiation-related protein or perilipin 2 (ADRP) all increase during adipogenesis (Yamaguchi et al., 2004; Zimmermann et al., 2004). We tested the hypothesis that invadolysin levels might also change during adipogenesis by examining murine 3T3-L1 and human SGBS (Green and Kehinde, 1976; Wabitsch et al., 2001; Cobbe et al., 2009) *in vitro* adipogenesis models. The process of adipogenesis is initiated by sequential activation of numerous transcription factors which act downstream of signaling pathways in response to intracellular or extracellular stimuli (Rosen and MacDougald, 2006). Insulin signaling plays a critical role in promoting lipid accumulation and energy storage (Imamura et al., 2002). Not surprisingly, insulin signaling is also important for adipogenesis. The loss of the IRS (insulin receptor substrate), inhibition of PI3K, Akt and mTOR (a direct target of Akt) have all been shown to inhibit adipogenesis (Sakaue et al., 1998; Kim and Chen, 2004; Lawrence et al., 2004; Tseng et al., 2004; Rosen and MacDougald, 2006).

The mechanism of invadolysin's localization to lipid droplets and its precise function there still remains unknown. In the present study, we have utilized *invadolysin* mutants to demonstrate a role for invadolysin in insulin signaling in *Drosophila*. We additionally used a starvation/refeeding model to demonstrate that Protein Kinase C activity is important for the localization of invadolysin to nascent lipid droplets. And finally, by utilizing two *in vitro* adipocyte differentiation systems, we demonstrated that the invadolysin increases during adipogenesis.

Results

We previously demonstrated that invadolysin localized to lipid droplets (LDs) by immunofluorescence of cultured cell lines and biochemically by immunoblotting fractionated A375 cells (a human melanoma cell line) (Cobbe et al., 2009). Reduction in fat body thickness and cell cross-sectional area, coupled with a decreased triglyceride : protein ratio in *invadolysin* mutant larvae indicated that invadolysin was functionally involved in lipid accumulation. We therefore set out to determine whether other parameters of metabolism were disrupted in *D. invadolysin* mutants.

Analysis of autophagy, glycogen accumulation and triglyceride storage

Insulin signaling positively regulates fatty acid and glycogen synthesis, and negatively regulates autophagy via the TOR (target of rapamycin) kinase (Halse et al., 2001; Jung et al., 2010; Wong and Sul, 2010). LysoTracker staining is a standard assay to detect autophagy (Munafó and Colombo, 2001; Chikte et al., 2014). In *Drosophila*, the fat body is the main lipid storage tissue and major energy reserve, similar to mammalian adipocytes. Staining of the fat body from control and *invadolysin* mutant larvae with LysoTracker demonstrated that autophagy was increased in *invadolysin* mutants (Figure 1A). We also show that the glycogen : protein ratio was significantly reduced in *invadolysin* mutants compared to wild type larvae, consistent with a role for invadolysin in insulin signaling (Figure 1B).

Feeding wild type *Drosophila* larvae a high sucrose diet significantly increases the triglyceride content (Musselman et al., 2011). To test if the ability to accumulate triglyceride was impaired in *invadolysin* mutants, animals were fed a high sucrose diet. On a high sucrose diet, wild type larvae had a significantly higher triglyceride : protein ratio than on a control diet (Figure 1C). *Invadolysin* mutant larvae on the other hand had a decreased triglyceride : protein ratio on a high sucrose diet compared to a control diet (Figure 1C). Decrease of the triglyceride : protein ratio in *invadolysin* mutant larvae fed a high sucrose diet suggested that the ability to synthesize or accumulate triglyceride was impaired in *invadolysin* mutants. Our data support the reported contention of antagonistic controls on autophagy and glycogen accumulation (Wang et al., 2001; Zirin et al., 2013).

In vertebrates, triglyceride storage is regulated by conserved lipases and LD associated proteins, such as perilipin. Perilipin, whose expression and activity are regulated by insulin, can promote LD formation (Prusty et al., 2002; Holm, 2003; Akimoto et al., 2005; Vereshchagina and Wilson, 2006). Lsd2, the *Drosophila* homologue of perilipin, localizes to LDs when ectopically expressed as a GFP-fusion (Miura et al., 2002). We hypothesized that the expression of Lsd2 might be altered in *invadolysin* mutants. Indeed, protein extracts from 96 h larvae showed that the Lsd2 level was decreased in *invadolysin* extracts relative to wild type, with a 2.5-fold decrease in 96 h *invadolysin* mutants (Figure 2A, B). The level of Lsd2 RNA was also decreased to 80% of the wild type level, suggesting control predominantly at the level of translation (data not shown).

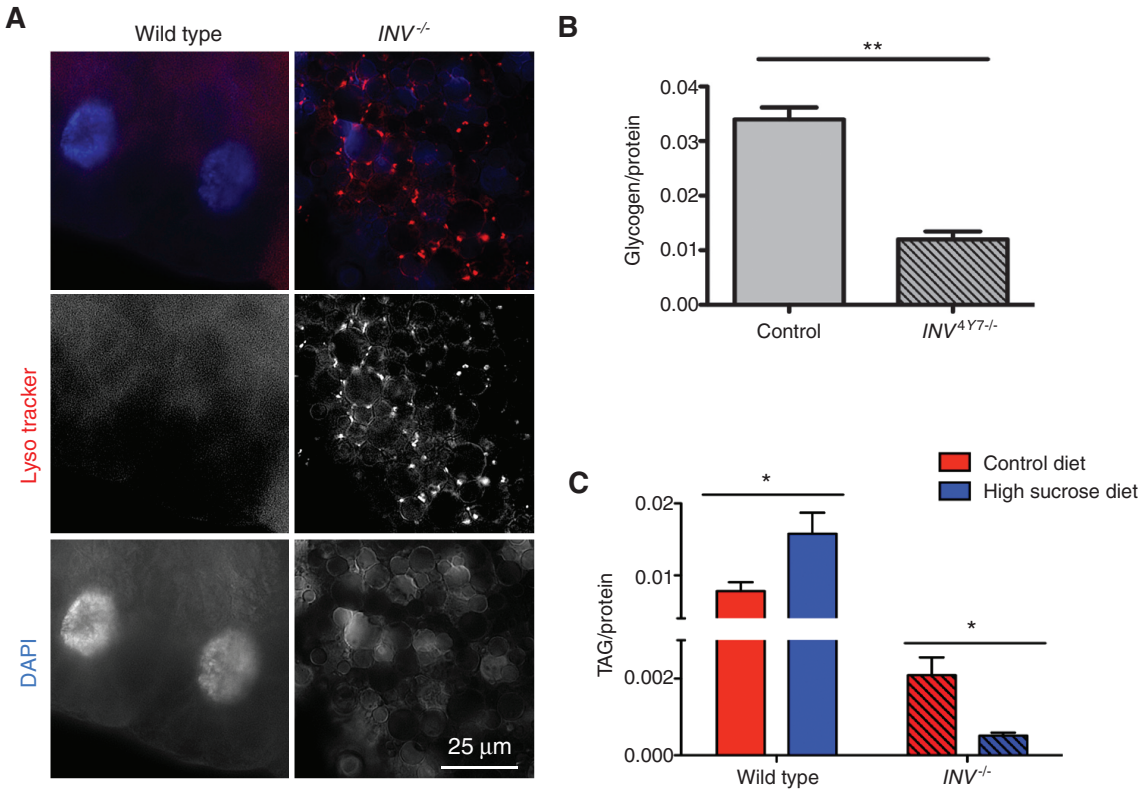

Figure 1: Metabolic consequences in *invadolysin* mutants.
(A) Staining of fat body with LysoTracker from wild type and *invadolysin* mutant (INV^{4Y7}) third instar larvae demonstrated that autophagy was increased in mutants compared to wild type. The images were captured at the same magnification. (B) The glycogen : protein ratio was significantly reduced in INV^{4Y7} mutant larvae compared to wild type larvae (data was analyzed by one-way ANOVA, $^{**}p < 0.01$). (C) On a high sucrose diet, control larvae accumulate significantly higher amounts of triglyceride whereas INV^{4Y7} mutants are unable to accumulate triglyceride on a high sucrose diet (data was analyzed by one-way ANOVA, $^{*}p < 0.05$).

Insulin signaling is impaired in *invadolysin* mutants *in vivo*

Multiple signaling pathways either positively or negatively regulate adipogenesis (Farmer, 2006). Of these, insulin signaling (initiated upon binding of insulin to its receptor) plays a critical role in promoting lipid accumulation and energy storage. To examine whether the observed increase in autophagy and decrease in glycogen and triglyceride accumulation in *invadolysin* mutants were consequences of impaired insulin signaling, we examined markers of insulin signaling in third instar wild type and *invadolysin* mutant larval extracts. While the basal level of Akt (a downstream effector of InR) was unchanged in *invadolysin* mutants, pAkt levels were reduced in *invadolysin* mutants (Figure 2C, D). These data suggest that activation of Akt, a downstream mediator of insulin signaling, may be disrupted in *invadolysin* mutant larvae.

As pAkt was decreased in *invadolysin* mutant larvae, we further examined the TOR pathway for additional downstream consequences. Activated Akt normally phosphorylates TSC2, leading to activation of TOR kinase (Inoki et al., 2002; Manning et al., 2002; Potter et al., 2002). Active TOR phosphorylates S6K (p70 S6 kinase) and 4E-BP (a translational inhibitor), two critical downstream effectors (Fingar and Blenis, 2004). Knockdown of TOR in *Drosophila* has previously been shown to eliminate the phosphorylation of S6K and 4E-BP (Yang et al., 2006). We thus examined the levels of phosphorylated/activated S6K and 4E-BP in wild type and *invadolysin* mutant larvae. We observed significantly reduced levels of pS6K (Figure 2E, F) and p4E-BP (Supplementary Figure 1) in *invadolysin* mutant extracts relative to wild type. Due to the decrease in the downstream pS6K and p4E-BP effectors, we hypothesize that invadolysin normally plays a positive regulatory role in promoting insulin signaling.

The activation of Akt upon insulin signaling also leads to the phosphorylation of the FOXO transcription factor, leading to the inhibition of 4E-BP expression (Teleman et al., 2005). As pAkt was decreased in *invadolysin* mutant larvae, we hypothesized that the expression of d4E-BP in *invadolysin* mutants might be increased. Consistent with

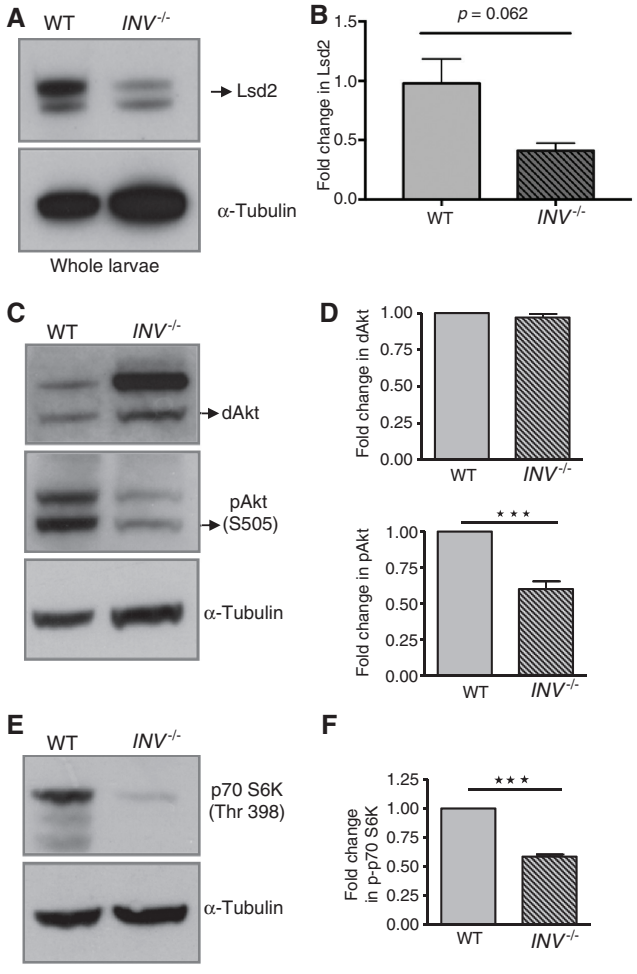

Figure 2: Loss of invadolysin resulted in impaired insulin signaling *in vivo*.

Extracts prepared from third instar wild type or *INV*^{4Y7} mutant larvae were immunoblotted for Lsd2, Akt, pAkt, and p70 S6K (downstream components of insulin signaling). Quantification of protein levels are shown in panels (B, D, F). (A, B) Immunoblotting demonstrates Lsd2 was decreased in *invadolysin* mutant whole larval extracts. (C, D) Immunoblot for Akt and activated pAkt in wild type (Canton S) and *INV*^{4Y7} larvae. The phospho-form of Akt was decreased, though not the unphosphoryated form. (E, F) Immunoblot for p70 S6K in wild type and *INV*^{4Y7} larvae. These data reveal decreased Lsd2, pAkt and p70 S6K in *INV*^{4Y7} mutant extracts.

this hypothesis, the level of 4E-BP mRNA was elevated in *invadolysin* mutant larvae (Supplementary Figure 1). Collectively, our data demonstrate that upon mutation of *invadolysin*, the phosphorylation of Akt, S6K and 4E-BP are all decreased, while 4E-BP appears to be increased (at least at the transcript level).

In summary, phosphorylated Akt, S6K and 4E-BP (the downstream mediators of insulin signaling) were all decreased in *invadolysin*. Downstream targets of the insulin/TOR pathway were also affected: autophagy (as a negative target) was increased, while glycogen and triglyceride accumulation (positive targets) were decreased in *invadolysin* mutants. Our results indicate that the insulin signaling pathway is impaired in *invadolysin* mutants.

Serum starvation/refeeding to examine the dynamics of invadolysin localization to LDs

We wanted to determine whether the presence of invadolysin on LDs was dynamic and responsive to insulin stimulation. Serum starvation/refeeding (a model for insulin stimulation) of cultured vertebrate cell lines leads to disruption of LDs followed by *de novo* LD formation (Ozeki et al., 2005; Andersson et al., 2006). A375 melanoma cells were starved overnight and then re-fed with serum-containing medium to stimulate LD reformation (Figures 3 and 4A). Under normal cell culture conditions, BODIPY staining of LDs and counterstaining with invadolysin antibody revealed invadolysin 'rings' on the surface of LDs (Figures 3 and 4A). Upon serum starvation, neither LDs nor invadolysin 'rings' could be detected. Within 30 min of serum re-feeding, LDs encircled by invadolysin were observed. These structures reached pre-starvation levels by 3 h of serum re-feeding. Cells containing 5 or more BODIPY foci were identified as LD-positive cells, while those containing 5 or more invadolysin foci were identified as invadolysin-positive cells (Figure 4B). LD- and invadolysin-positive cells increased with the length of time in fresh serum-containing medium. 50% of cells were LD/invadolysin-positive after 1 h incubation, rising to 100% after 3 h re-feeding. These results suggest that invadolysin localized to LDs coincident with LD formation. The coincident appearance of invadolysin on LDs could result either from invadolysin recruitment to LDs or *de novo* synthesis of invadolysin. As shown in the immunoblots of Figure 4C, the level of invadolysin did not dramatically change after starvation. Invadolysin was also recruited to newly formed LDs following pretreatment of cells with 10 μM cycloheximide for 1 h before refeeding (data not shown), suggesting that the localization of invadolysin to LDs was not dependent on *de novo* protein synthesis. We hypothesize that starvation resulted in the dispersal of invadolysin into the cytoplasm, which was then recruited to newly-formed LDs upon serum feeding.

Protein kinase C requirement for the localization of invadolysin to newly synthesized LDs

Several proteins related to cell signaling such as protein kinase C (PKC) δ, diacylglycerol kinase (DGK) δ, PKA, Ras,

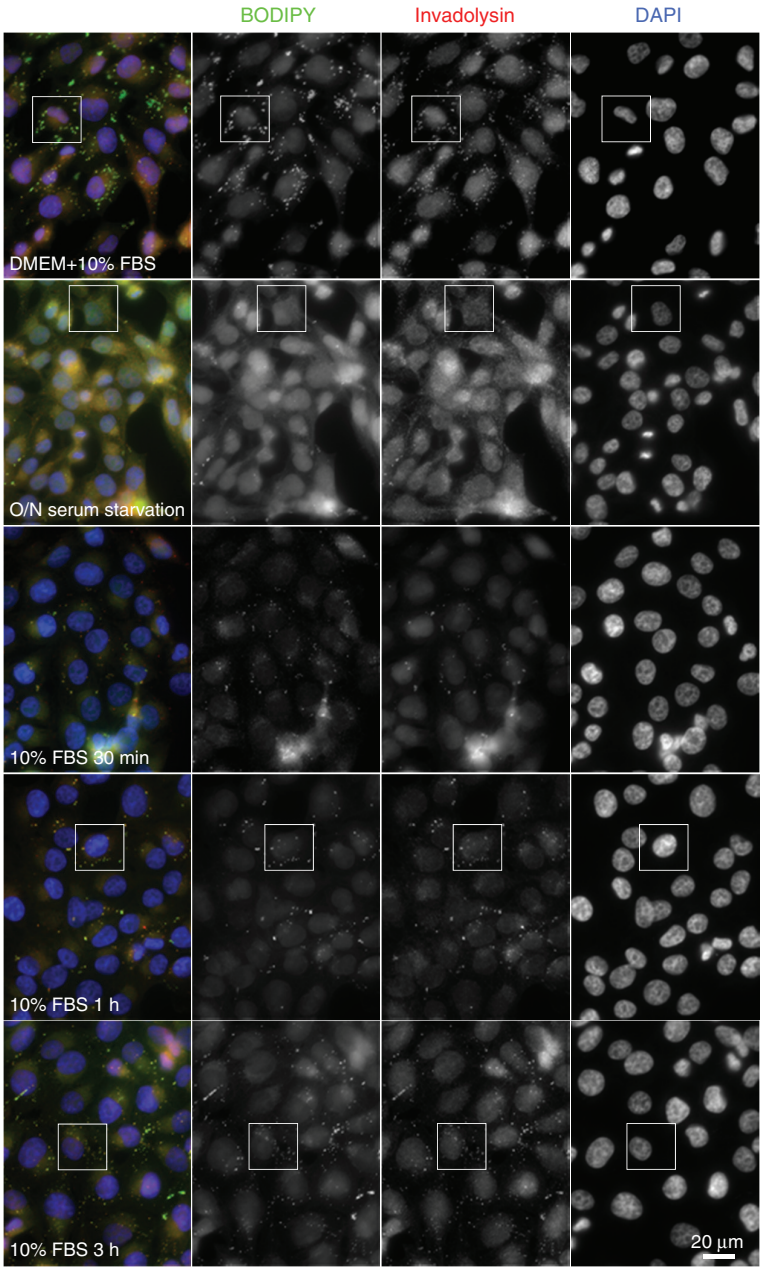

Figure 3: Invadolysin was recruited to newly formed LDs.
Human A375 melanoma cells were starved in serum-free medium overnight, and then fed fresh medium containing 10% FBS. Cells were fixed and stained for LDs (green), invadolysin C-Ab1 (red) and DNA (blue). Neither LDs nor invadolysin foci were detectable following serum starvation. However, both LDs and invadolysin rings were clearly observed after cells were incubated in fresh medium containing 10% FBS. Higher magnifications of the areas enclosed by the white boxes are shown in Figure 4A. Scale bar = 20 µm.

Raf and P-MAPK have been shown by proteomic analysis to localize to LDs (Turro et al., 2006). PKC α and PKC δ can additionally translocate to LDs after stimulation of RAW 264.7 macrophages with oleic acid (Chen et al., 2002).

To address whether PKC plays a role in the localization of invadolysin during the *de novo* generation of LDs, the general PKC inhibitor, Ro31-8220, was added during the starvation/refeeding experiment. A375 cells were starved for 24 h to disrupt LDs, and then treated with 5 µM Ro31-8220 for 1 h. Cells were refed for another 3 h in fresh medium containing Ro31-8220, and subsequently analyzed for invadolysin and LDs. DMSO alone had no effect on invadolysin dispersal and relocalization (Figure 5A). However, PKC inhibition disrupted the localization of invadolysin, with the majority of invadolysin appearing as cytosolic aggregates distinct from LDs (Figure 5B).

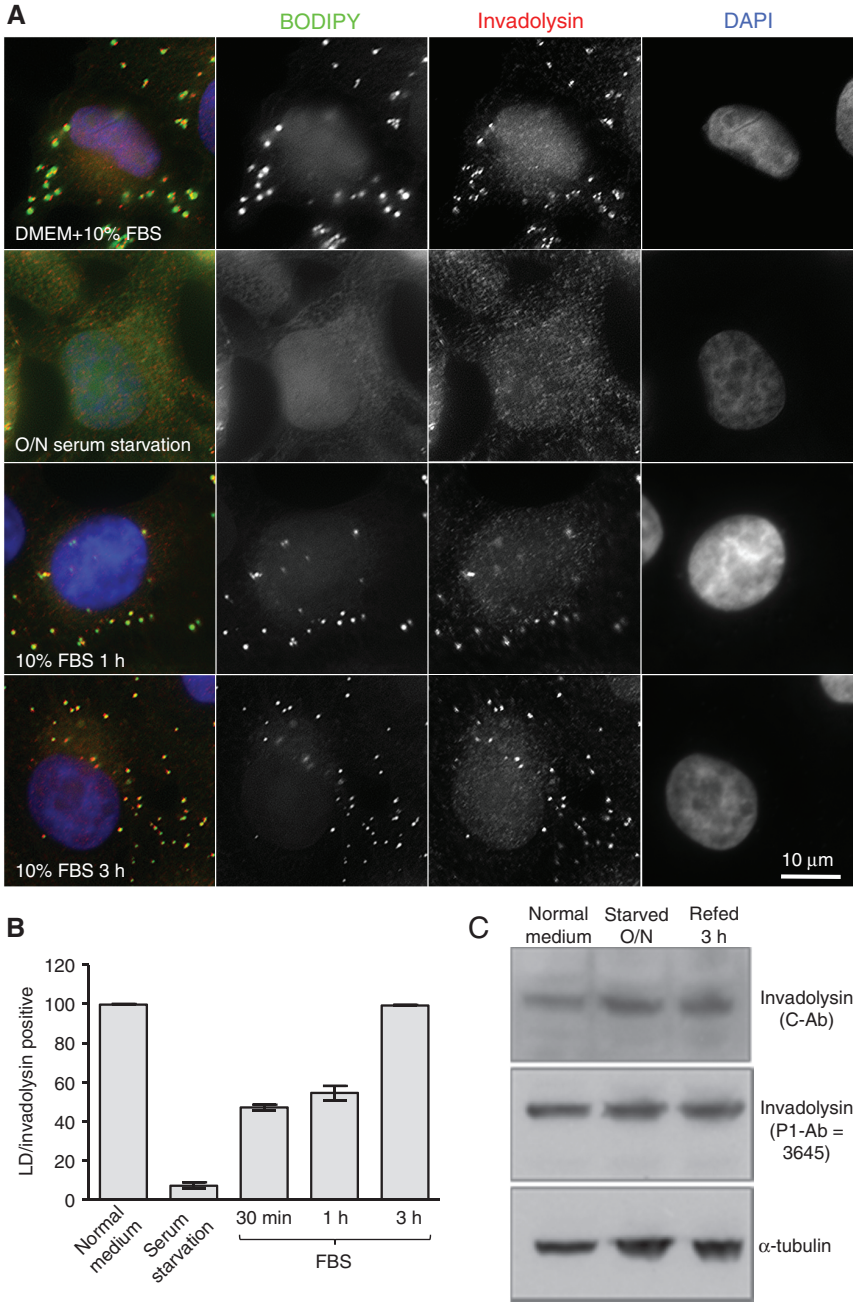

Figure 4: LDs containing invadolysin increased after refeeding of starved cells.
(A) Three-fold higher magnification of the areas enclosed by white boxes in Figure 3. LDs and invadolysin could not be detected following serum starvation, but were clearly observed after cells were incubated in fresh serum-containing medium. Scale bar = 10 µm. (B) Quantitation of LDs following refeeding of starved A375 cells. Cells containing five or more BODIPY foci were identified as BODIPY-positive. The graph shows the mean value and standard deviation (SD) from 3 independent experiments where 400–500 cells were counted for each time point. LD-positive cells reached pre-starvation levels in 3 h. (C) Protein extracts were prepared from cells cultured in: medium containing 10% FBS, serum-free medium (overnight), and fresh serum-containing medium (for 3 h). Invadolysin was detected by immunoblotting using invadolysin 3646 and C-Ab1 antibodies (Cobbe et al. 2009, and Figure 9).

Although LDs still formed when PKC was inhibited, 'rings' of invadolysin were rarely observed. These data suggest that the localization of invadolysin to nascent LDs was dependent on PKC activity.

To determine whether invadolysin could relocalize to LDs after Ro31-8220 removal, A375 cells were starved and refed with fresh medium containing Ro31-8220 for 3 h. Cells were then incubated with fresh medium

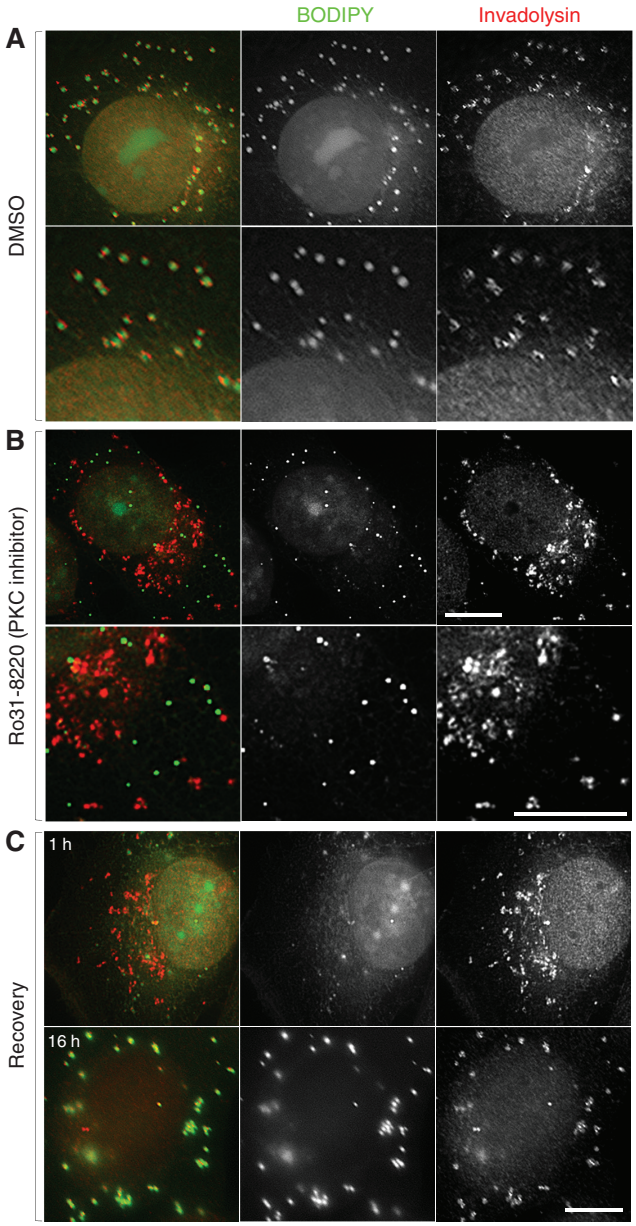

Figure 5: Inhibition of protein kinase C blocked recruitment of invadolysin to newly formed LDs.
A375 cells were starved in serum-free medium for 24 h. (A) 5 μM DMSO or (B) or Ro31-8220 was added to inhibit PKC activity. After 1 h, cells were refed with fresh medium containing 10% FBS and Ro31-8220 and incubated for another 3 h. (A) DMSO does not affect the localization of invadolysin to LDs. (B) Upon Ro31-8220 treatment, invadolysin formed aggregates that were distinct from LDs. (C) Relocalization of invadolysin to LDs after removal of PKC inhibitor Ro31-8220. A375 cells were treated as in A, but medium lacking Ro31-8220 was added after 3 h. Cells were stained for LDs (green) and invadolysin (red).

lacking Ro31-8220. While aggregates of invadolysin were still observed in cells 1 h after removal of Ro31-8220, after 16 h invadolysin was apparent on LDs (Figure 5C). This experiment suggested that PKC activity was important for invadolysin's localization to LDs.

Protein phosphorylation is a common post-translational modification used to regulate activity, localization, stability or molecular interactions (Bartz et al., 2007). As the localization of invadolysin to LDs appeared to be PKC-dependent, we analysed the sequence of invadolysin for evolutionarily conserved PKC phosphorylation sites by NetPhosK 1.0 (Blom et al., 2004), NetPhos 2.0 (Blom et al., 1999), and GPS2.1 (Xue et al., 2008). Four threonines (at positions 220, 269, 458 and 467) in the invadolysin sequence scored highly for potential PKC phosphorylation (Figure 6A).

To determine whether invadolysin may be phosphorylated by PKC *in vitro*, bacterially-expressed recombinant invadolysin fragments were affinity purified and an *in vitro* kinase assay performed. The nearly full-length 'GST-VINK' construct, as well as an N-terminal V1N construct were phosphorylated by protein kinase C *in vitro*, while the C-terminal V1C construct was not (Figure 6B, C). These results suggested phosphorylation site(s) within the first 300 amino acids of invadolysin. We postulate that T220 and/or T269 may be phosphorylated by PKC. Both of the corresponding residues in the leishmanolysin sequence map to the surface of the leishmanolysin structure (rather than to the interior of the protein). While T269 (V261 in leishmanolysin) lies in a pocket, T220 (S219 in leishmanolysin) is more exposed. We therefore predict that T220 in invadolysin is more likely to be phosphorylated by PKC.

The localization of invadolysin during murine 3T3-L1 adipogenesis *in vitro*

The *in vivo* data from *D. invadolysin* mutants, coupled with the serum starvation/refeeding model suggested that invadolysin may play a role in adipogenesis. Adipocyte differentiation is a multi-step process that requires growth inhibition by cell-to-cell contact and hormonal induction for mitotic clonal expansion, followed by accumulation of triacylglycerol storage in LDs (Rosen and Spiegelman, 2000). We decided to investigate invadolysin in two vertebrate *in vitro* adipogenesis systems.

To examine the level and localization of LD proteins during murine adipogenesis, 3T3-L1 cells were induced to differentiate into adipocytes and the subcellular localization of invadolysin and perilipin determined by immunofluorescence (Figure 7A). On day 2, invadolysin exhibited a punctate staining pattern in the cytosol. At day 4, the

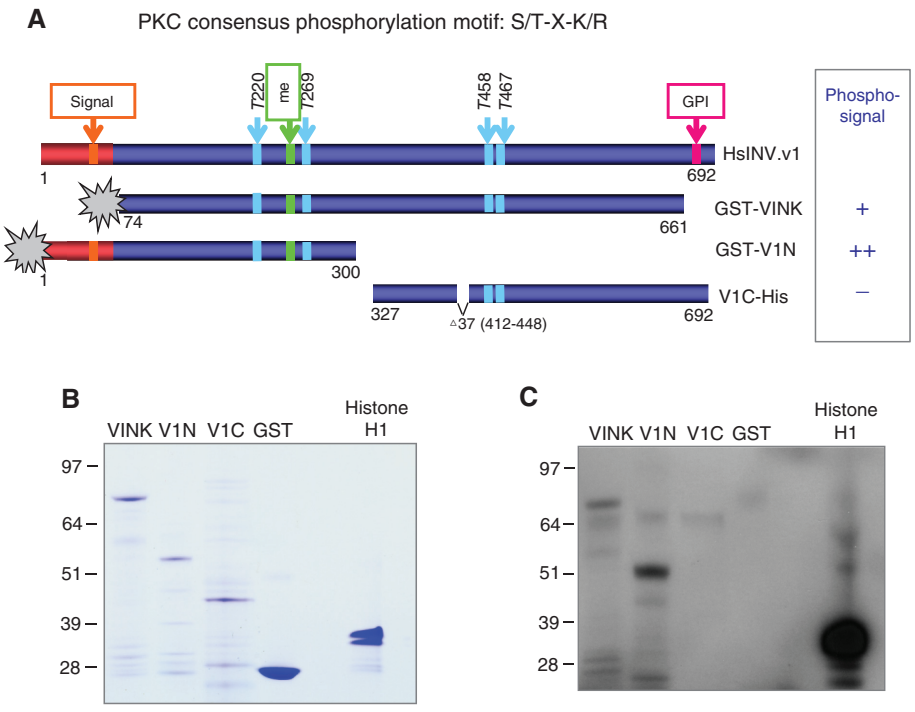

Figure 6: Invadolysin can be phosphorylated *in vitro* by protein kinase C.
(A) Schematic representation of human invadolysin, including predicted signal sequence (orange), metalloprotease (green), and GPI-addition (pink) sites. Putative PKC phosphorylation sites (blue arrows) and the truncated invadolysin constructs tagged with GST (gray) or [His]6 at the N-terminus are depicted. (B) Coomassie Brilliant Blue stained polyacrylamide gel shows the amount of protein used for the *in vitro* kinase assay. (C) Recombinant invadolysin proteins, GST (negative control) and Histone H1 (positive control) were incubated with PKC and γ-32P-ATP and then analyzed by 4–12% NuPAGE and autoradiography. GST-VINK and GST-V1N were phosphorylated by PKC *in vitro*, while V1C-His was not. These results demonstrate that one or more sites within the N-terminal half of invadolysin could be phosphorylated by PKC *in vitro*.

size of LDs increased and the cells acquired a circular morphology. Invadolysin displayed a cytoplasmic ring-like distribution at days 2 and 4. At day 6, invadolysin rings were not as apparent as at earlier times, and invadolysin appeared dispersed in the cytosol of fully differentiated adipocytes (day 8). These data suggest that invadolysin localized to LDs in the early stages of differentiation, but then disassociated from LDs at later stages. Perilipin showed a localization pattern distinct from invadolysin. Perilipin was strikingly localized in the nucleus on days 0–2 of differentiation (not previously described). However, from day 4 onward, a pronounced ring-like distribution surrounding LDs was observed (Figure 7A). With further culture until day 14 post-differentiation, small and large LDs were observed within the same 3T3-L1 adipocyte. Intriguingly, invadolysin appeared to preferentially encircle small rather than large LDs, whereas perilipin encircled every LD (Figure 7B). These results highlight the dynamic nature of LD proteins. Differential localization between invadolysin and perilipin may reflect different roles played by these proteins.

Invadolysin increases during 3T3-L1 adipogenesis

In order to determine whether invadolysin mRNA changes during 3T3-L1 differentiation, qRT-PCR was performed on RNA extracted from 3T3-L1 cells at different times (and normalized to actin). The relative expression at various time points was further normalized to day 0, in order to present the relative change of expression over time. TIP47 is the only PAT (Perilipin, ADRP and TIP47) protein that appears to be functionally unrelated to adipocyte differentiation (Yamaguchi et al., 2004), and its mRNA did not change significantly during adipogenesis (Figure 7C). On the other hand, invadolysin, ADRP and perilipin mRNA all increased to varying degrees during adipocyte differentiation (Figure 7C). Invadolysin mRNA increased gradually during differentiation reaching a 10-fold increase on day 8. ADRP mRNA increased close to 15-fold, while the expression of perilipin exhibited a dramatic 100-fold increase at day 2 and continued to increase to more than 250-fold at day 4.

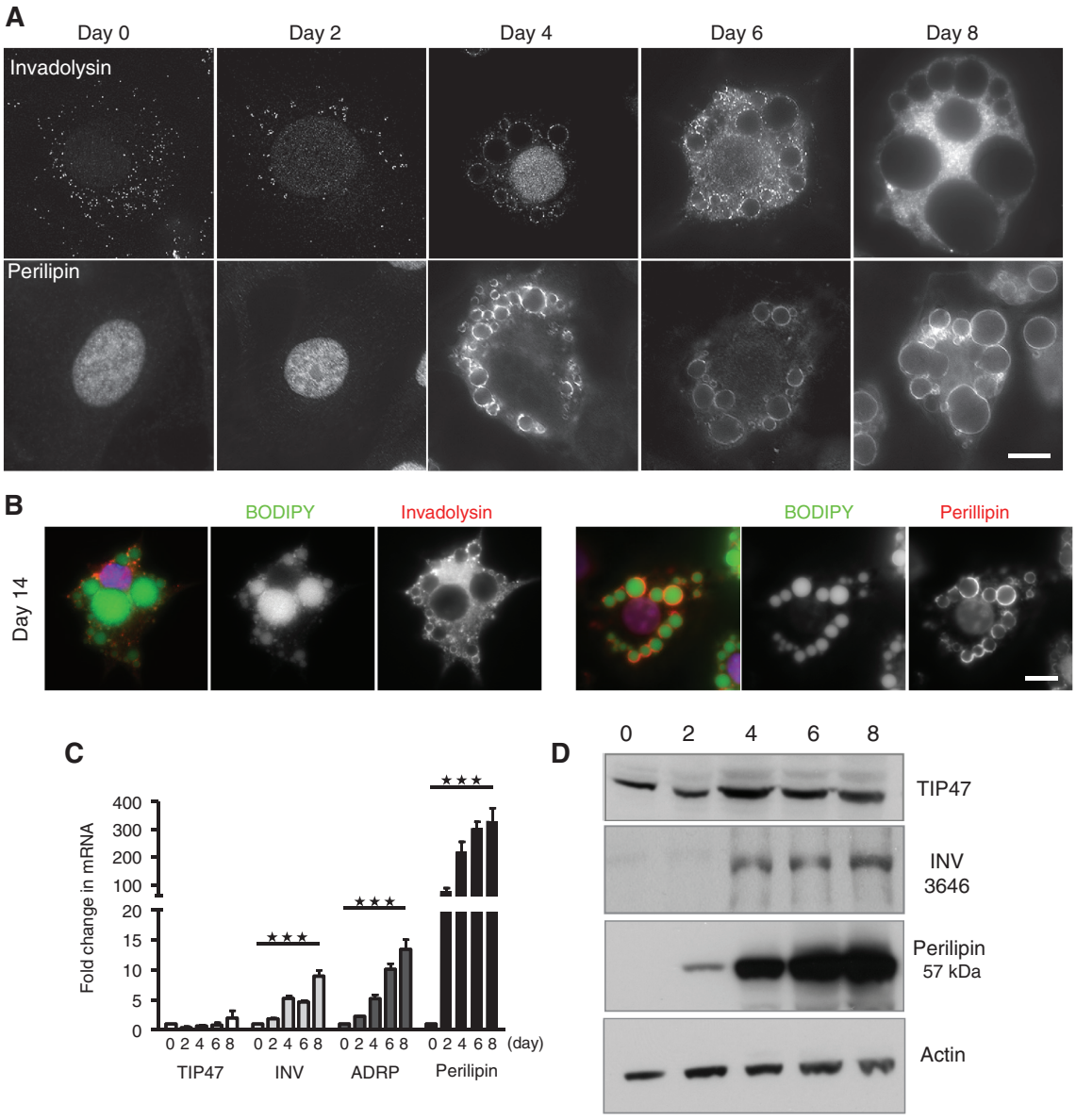

Figure 7: Determination of invadolysin localization and level during 3T3-L1 adipogenesis.
(A) At different time points in the differentiation protocol, 3T3-L1 cells were fixed and stained for invadolysin (upper) or perilipin (lower). In the early stages of differentiation (days 2 and 4), invadolysin was observed surrounding LDs. At day 8, invadolysin appeared dispersed in the cytosol of differentiated 3T3-L1 cells. Another LD binding protein, perilipin, was found surprisingly to localize in the nucleus at days 0–2. From day 4, perilipin encircled LDs. (B) Day 14 adipocytes were fixed and stained for LDs (green), DNA (blue), and invadolysin or perilipin (red). Invadolysin encircled smaller LDs, while perilipin surrounded all LDs. (C) Invadolysin mRNA increased significantly during adipocyte differentiation. Total RNA from 3T3-L1 cells undergoing differentiation was analysed by qRT-PCR using appropriate primers and probes for the expression of TIP47, invadolysin, ADRP, and perilipin. The expression of each gene was normalized to actin and the fold-change of expression was normalized to day 0. Each experiment was performed in triplicate. The graph shows the mean value and standard deviation (SD) for 3 independent experiments. For comparison the difference between each day was further analyzed by one-way ANOVA (nonparametric) in 95% confidence intervals (***$p < 0.0001$). (D) The expression of invadolysin and perilipin (but not TIP47) increased during adipogenesis. Cell lysates from different days during differentiation were prepared. Protein expression was detected by immunoblotting using designated antibodies.

As invadolysin mRNA increased during adipocyte differentiation, it was important to address whether the level of the protein also increased. We compared invadolysin protein with other PAT proteins during differentiation. While the amount of TIP47 did not change during differentiation, we observed a dramatic increase in both invadolysin and perilipin upon adipocyte differentiation (Figure 7D). These results thus demonstrate a correlation

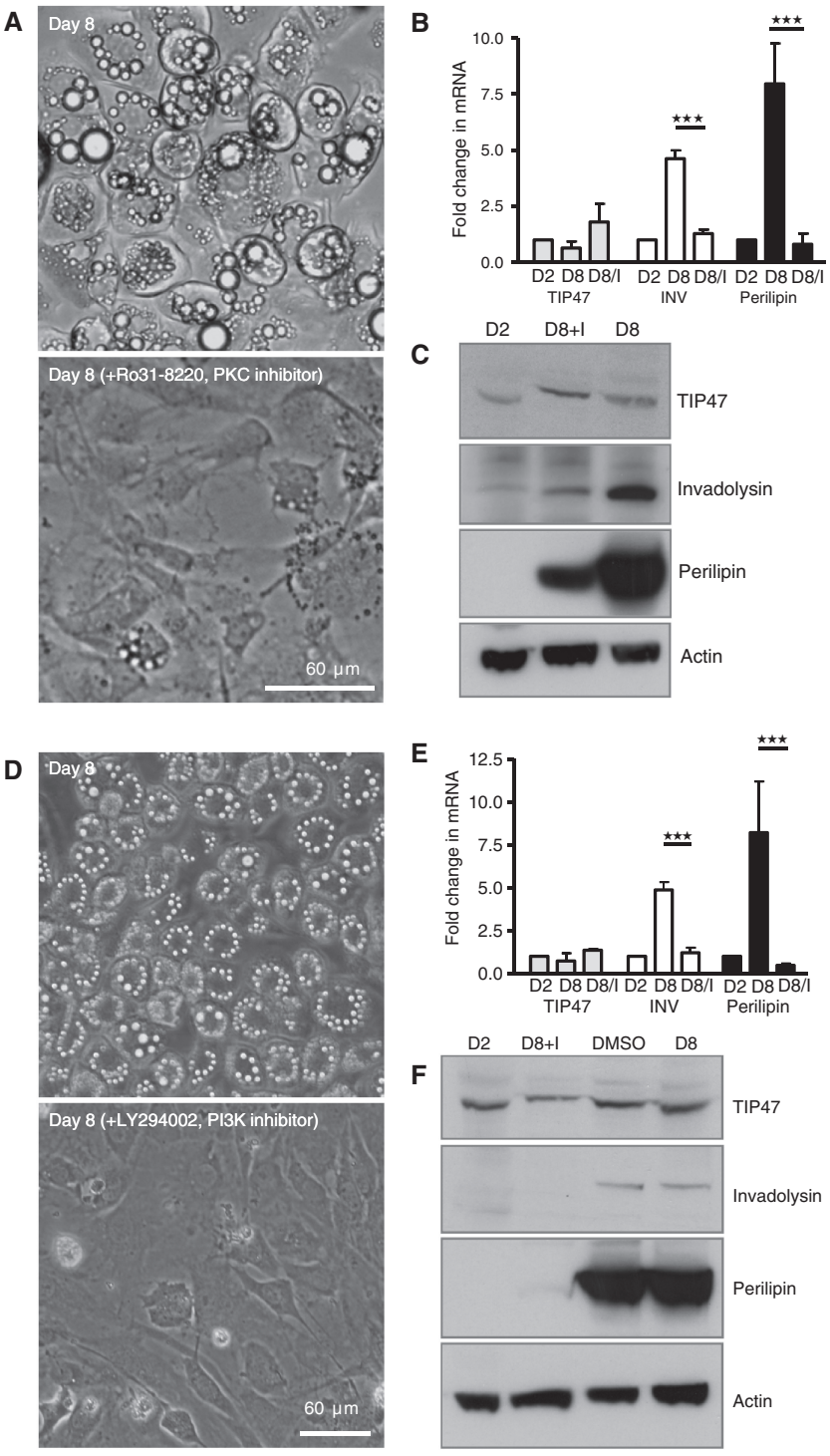

Figure 8: Invadolysin and perilipin mRNA and protein decreased when PKC or PI3K were inhibited.
3T3-L1 cells were induced to differentiate into adipocytes. On day 2, either 5 µM Ro31-8220 (a PKC inhibitor) or 50 µM LY294002 (a PI3K inhibitor) was added to cells and the culture medium was replaced with fresh inhibitor-containing medium every 2 days until day 8. A–C) Inhibition of adipocyte differentiation was observed after inhibition of PKC, while the effects of PI3K inhibition are shown in panels (D)–(F). (A and D) Scale bar = 60 µm. (B and E) mRNA expression of TIP47, invadolysin, and perilipin was quantified by qRT-PCR. The expression of each gene was normalized to actin and the fold change of expression was normalized to day 2. Data are representative of three individual experiments and each experiment was performed in triplicate. The graphs show the mean value and standard deviation (SD) for three independent experiments. For differential comparisons, the data were further analyzed by one-way ANOVA (nonparametric) at 95% confidence intervals (***$p < 0.0001$). (C and F) Cell lysates were collected on the days indicated. '+I' indicates treatment with the PKC or PI3K inhibitor. TIP47, invadolysin, perilipin and actin were detected by immunoblotting.

between invadolysin level and progression of 3T3-L1 adipogenesis.

Inhibition of PKC and PI3K blocked 3T3-L1 adipogenesis and the elevation of invadolysin and perilipin

A number of studies have suggested that PKC may regulate adipocyte differentiation (Fleming et al., 1998; Zhou et al., 2006). While our results showed that the invadolysin level did not dramatically change between days 0–2 of adipogenesis, a significant increase was observed between days 2 and 4. Therefore, after induction of differentiation by IBMX/DEX/insulin on day 0, the broad-spectrum PKC inhibitor Ro31-8220 was added to cells on day 2 and incubated until day 8. mRNA and protein extracts were prepared before inhibitor treatment on day 2, and on day 8 (with and without inhibitor treatment), and analyzed for TIP47, INV, perilipin, and actin. In control 3T3-L1 cultures, most cells differentiated into mature adipocytes by day 8. However, when PKC was inhibited, cells failed to differentiate (Figure 8A). Consistently, the mRNA and protein levels of invadolysin and perilipin were decreased in Ro31-8220-treated cells, whereas TIP47 expression level did not change when adipocyte differentiation was blocked (Figure 8B, C).

We examined the effects on adipogenesis after treating cells with a PI3K inhibitor (LY294002) as PI3K is an important mediator of insulin's effects (Rosen and MacDougald, 2006; Tseng et al., 2004). LY294002 was added at day 2 till day 8 to block adipocyte differentiation (Figure 8D), and mRNA and protein extracts were prepared from cells on these days. When PI3K was inhibited, adipocyte differentiation was blocked (Figure 8D), and the mRNA and protein levels of invadolysin and perilipin were decreased (Figure 8E, F). The expression of TIP47 mRNA was unaffected by inhibition of PI3K. These data demonstrate that when adipogenesis was blocked by treatment with PKC or PI3K inhibitors, invadolysin and perilipin do not increase.

Invadolysin also increased during human SGBS adipogenesis *in vitro*

SGBS cells are a human preadipocyte cell line derived from subcutaneous white adipose tissue of a patient suffering from Simpson-Golabi-Behmel syndrome (SGBS), an X-linked disorder caused by mutation in the *glypican-3* gene (Xuan et al., 1999; Wabitsch et al., 2001). As invadolysin increased during murine 3T3-L1 adipogenesis, we set out to determine if invadolysin also increased during human SGBS differentiation.

We have detected four alternatively-spliced variants of invadolysin in human cells (Cobbe et al., 2009), depicted in Figure 9A. The N-terminal variants of INV, INV.v1 and INV.v2 use an alternate reading frame. Each of the two N-terminal variants also has an alternatively spliced version (+37 and Δ37), with or without the 37 amino acids encoded by exon 12. There was no detectable change by RT-PCR in the transcript levels of these variants during SGBS differentiation (Figure 9B–E). INV.v1+37 was the most prevalent variant at all time points analysed. Interestingly, this variant most closely resembles the single variant expressed in *Drosophila*. The RT-PCR results differ from the qPCR results obtained for 3T3-L1 cells (Figure 7C), likely reflecting sensitivity differences in the techniques.

The morphological changes during SGBS adipogenesis are shown in Figure 10A. Over time, cells fill with LDs, and the nuclei become compressed in appearance. As with 3T3-L1 cells, invadolysin protein increased during SGBS adipogenesis (Figure 10B). Utilizing antibodies generated against different invadolysin peptides (to examine distinct variants) demonstrated that translation of invadolysin variants may be regulated during adipogenesis. Antibody 3645/6 was raised against a sequence common to all predicted human invadolysin variants (Figure 9A), upstream of the metalloprotease motif. While the level of a 52 kDa form of invadolysin (that we postulate to be a processed form) remained constant during adipogenesis, the level of a larger 66 kDa form of invadolysin increased during SGBS adipogenesis (Figure 10B). The 66 kDa form was similar to the predicted full-length size of invadolysin (Table 1).

Examining the distinct INV.v1 and INV.v2 N-terminal variants demonstrated additional regulation. Antibodies 4624 and 4888 were designed against distinct peptide sequences of the INV.v1 and INV.v2 variants, respectively (Figure 9A). The 4624 antibody bound to a 39 kDa band that may represent a cleaved region from the N-terminus of INV.v1 (Figure 10C). Blotting with 4888 (INV.v2) showed the level of a 52 kDa form to remain constant, while a 66 kDa form of INV.v2 increased during adipogenesis (Figure 10D). The patterns observed with the 3646 and 4888 antibodies were strikingly similar, suggesting that the 52 and 66 kDa forms of invadolysin may both derive from INV.v2 translation. Table 2 summarizes the change in protein levels of different forms of invadolysin. Increase of

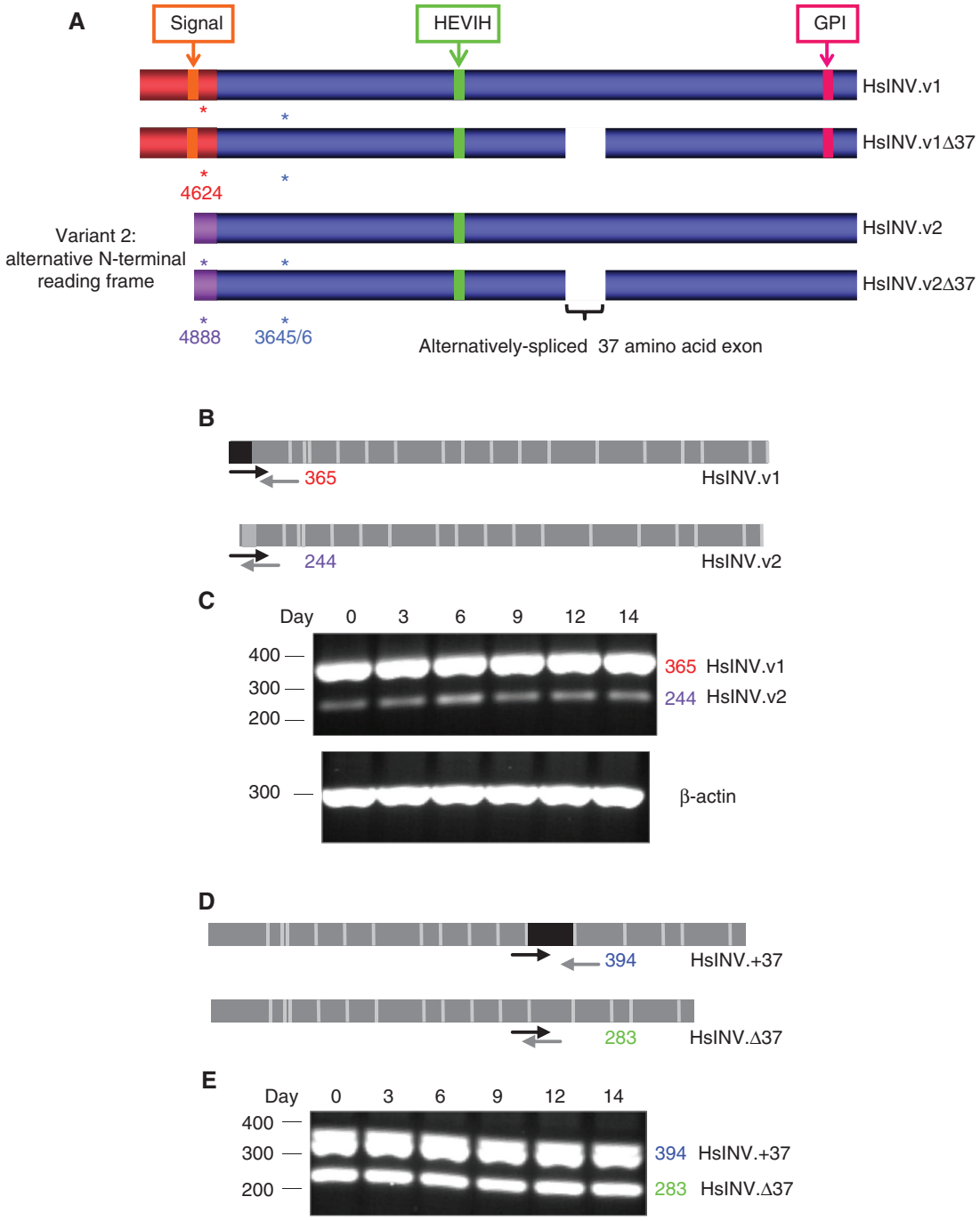

Figure 9: Analysis of invadolysin alternatively-spliced variants during SGBS adipogenesis.
(A) Schematic of the four alternative splice variants of human invadolysin. The asterisks highlight the locations of the peptides used to elicit the 4624, 4888, and 3645/3646 antibodies. The peptide sequence for 3645/3646 is common to all variants thus this antibody should recognize all expressed variants. Antibodies 4624 and 4888 recognize INV.v1 and INV.v2, respectively. (B) Schematic representing transcripts of the two alternatively-spliced N-terminal variants of human invadolysin and the location of primers Hv2f and Hv2r with the predicted size of RT-PCR amplicons. (C) RT-PCR using Hv2f and Hv2r demonstrates that transcripts for INV.v1 and INV.v2 are present and do not appear to change appreciably throughout SGBS adipogenesis (though INV.v1 is more prevalent). (D) Schematic representing alternatively-spliced exon 12 INV.+37 and INV.Δ37 variants of human invadolysin and the location of primers H12f and H12r flanking exon 12 with the predicted size of RT-PCR amplicons. (E) RT-PCR using primers H12f and H12r demonstrates that transcripts for the INV.+37 and INV.Δ37 variants are present and do not appear to change appreciably throughout SGBS adipogenesis (though the INV.+37 variant is more prevalent). The most common RNA species based on this analysis is HsINV.v1+37.

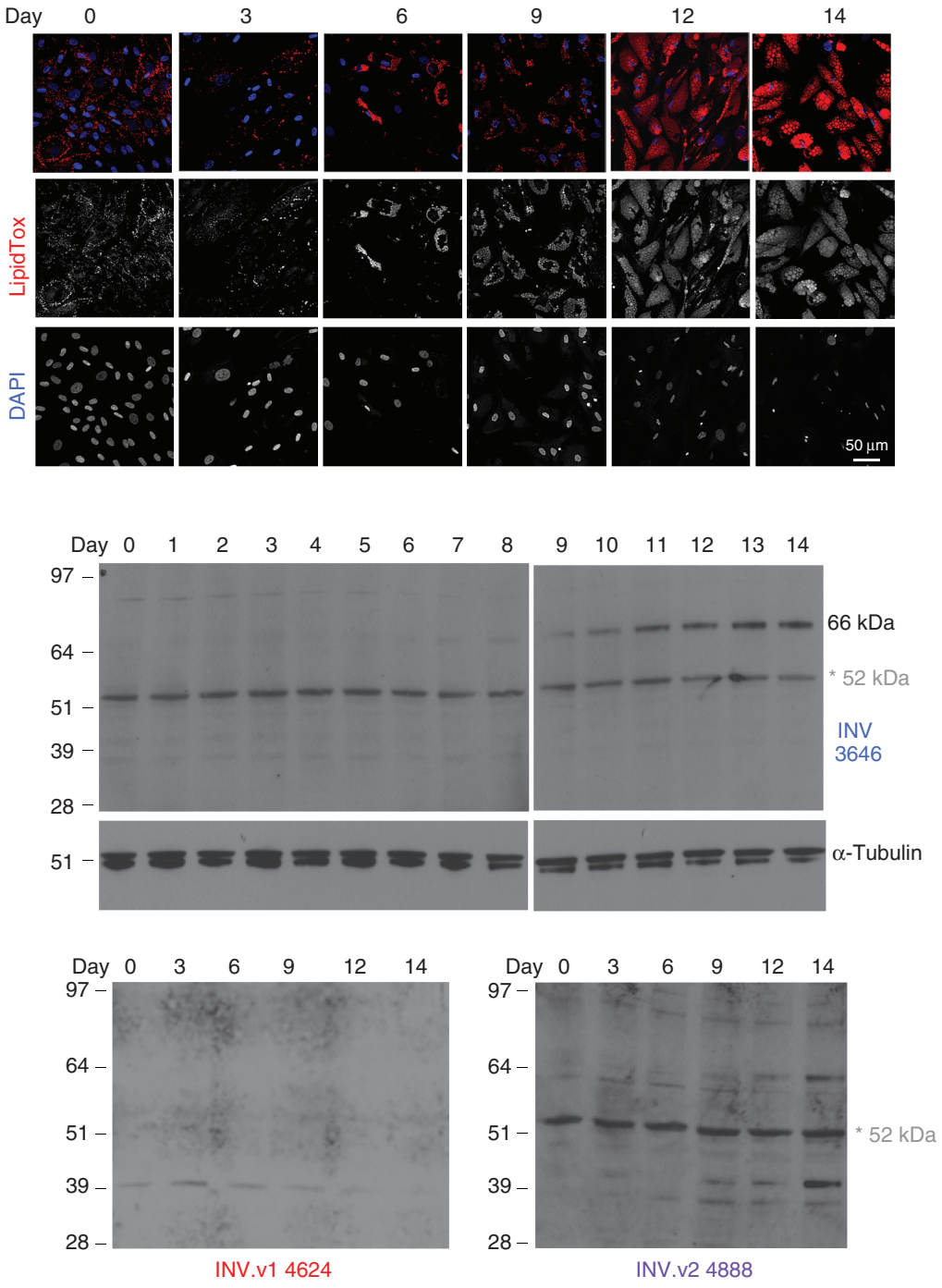

Figure 10: Invadolysin increased during adipogenesis of SGBS cells.
(A) Images of SGBS cells stained for LDs with LipidTox (red) and DNA with DAPI (blue) at time points during adipogenesis. Scale bar = 50 µm. (B) Protein extracts at different time points were probed with the 3646 invadolysin antibody. Immunoblotting showed that a 66 kDa form of invadolysin increased from day 8 of adipogenesis, while the level of a 52 kDa form of invadolysin did not change (*the 52 kDa band is detected by the secondary antibody alone and therefore unrelated to invadolysin). The 66 kDa form of invadolysin is close to the predicted full-length form (Table 1). (C) Immunoblotting of protein extracts from different time points with 4624 detected a 39 kDa band during adipogenesis. The 39 kDa band may represent a pro-region cleaved from INV.v1. (D) Immunoblotting of extracts with 4888 demonstrated an increase in 39 and 66 kDa forms of INV.v2 (* the 52 kDa band is detected by the secondary antibody alone and therefore unrelated to invadolysin).

Table 1: Predicted molecular weight of invadolysin variants.

Alternative splice variant	Number of amino acids (unprocessed)	Predicted mol. weight (kDa)
HsINV.v1	692	78.12
HsINV.v1Δ37	655	73.58
HsINV.v2	640	72.79
HsINV.v2Δ37	603	68.25

The predicted molecular weights (Sequence manipulation suite) of the different alternatively-spliced variants of human invadolysin are based on the amino acid sequence. Invadolysin variant INV.v1 contains a predicted signal sequence, and 37 amino acid exon 12. It has the highest predicted (unprocessed) molecular weight of 78.12 kDa. The variant INV.v2Δ37 lacks a signal sequence and exon 12. This variant has the lowest predicted (unprocessed) molecular weight amongst the four variants, at 68.25 kDa. As any potential processing of invadolysin has yet to be defined, it has not been included in these measurements.

the INV.v2 66 kDa protein suggests a potential role for this form during SGBS adipogenesis *in vitro*.

Inhibition of PI3K blocked the increase in invadolysin during SGBS adipogenesis

To further examine the correlation between invadolysin increase and adipogenesis, we inhibited adipogenesis by blocking PI3K and TOR kinase, two downstream mediators of insulin signaling (El-Chaâr et al., 2004; Aubin et al., 2005). We used wortmannin and LY29004 to inhibit PI3K, and rapamycin to inhibit TOR kinase (Figure 11A) (Vlahos et al., 1994; Norman et al., 1996; Oshiro et al., 2004). Blocking PI3K prevented the increase of the 66 kDa form of invadolysin, while the 52 kDa form was unchanged (Figure 11B [3646]). Blocking TOR kinase resulted in an intermediate impact on the 66 kDa band, but not on the 52 kDa band (Figure 11B [3646]). Similar results were observed when probing for INV.v2 (Figure 11B [4888]): the 52 kDa and 66 kDa forms of invadolysin were decreased upon inhibition of PI3K, but less so by inhibition of TOR kinase.

Akt lies downstream of PI3K in the insulin-signaling cascade and represents a critical node in the pathway (Taniguchi et al., 2006). A decrease in pAkt was observed upon PI3K inhibition, demonstrating that the insulin pathway was indeed impaired. TOR kinase inhibition did not affect the pAkt level, as TOR lies downstream of Akt. These results suggest that the change in INV.v2 may be effected downstream of PI3K, but upstream of TOR. Our results further strengthen the hypothesis that invadolysin may play an important role in adipogenesis.

Discussion

The *invadolysin* gene encodes a conserved metalloprotease of the M8 family. The loss of invadolysin in *Drosophila* results in late larval lethality and a range of pleiotropic phenotypes including defects in mitotic progression, cell migration and mitochondrial function as well as accumulation of nuclear envelope proteins and mono-ubiquitinated Histone H2B (McHugh et al., 2004; Di Cara et al., 2013; Rao et al., 2015). Invadolysin is localized to LDs, and *invadolysin* mutant larvae fail to accumulate triglycerides (Cobbe et al., 2009).

Herein we have demonstrated that insulin signaling is impaired in *D. invadolysin* mutants, with consequences on

Table 2: A qualitative summary for the change of invadolysin variant levels during SGBS adipogenesis.

Mol. weight of detected bands (kDa)	Day 0	Day 3	Day 6	Day 9	Day 12	Day 14
Antibody 3646: raised against a sequence common to all forms of invadolysin						
66	N/C	N/C	N/C	+	++	+++
[a]52	N/C	N/C	N/C	N/C	N/C	N/C
Antibody 4624: raised against a peptide sequence found only in INV.v1						
39	N/C	N/C	N/C	N/C	N/C	–
Antibody 4888: raised against a peptide sequence found only in INV.v2						
66	N/C	N/C	N/C	+	++	+++
[a]52	N/C	N/C	N/C	N/C	N/C	N/C
39	N/C	N/C	N/C	+	+	+++

The table summarizes the change in invadolysin variant levels as observed using different antibodies. 'N/C' indicates no observable change in variant level whereas '+' and '–' represent an increase and decrease in variant level, respectively. The 3646 antibody which is designed against a region common to all variants and the 4888 antibody which is designed against a region specific to INV.v2 show a similar pattern in the level of the 66 kDa form of invadolysin. [a]We have determined that the 52 kDa form is detected by the secondary antibody alone and therefore unrelated to invadolysin.

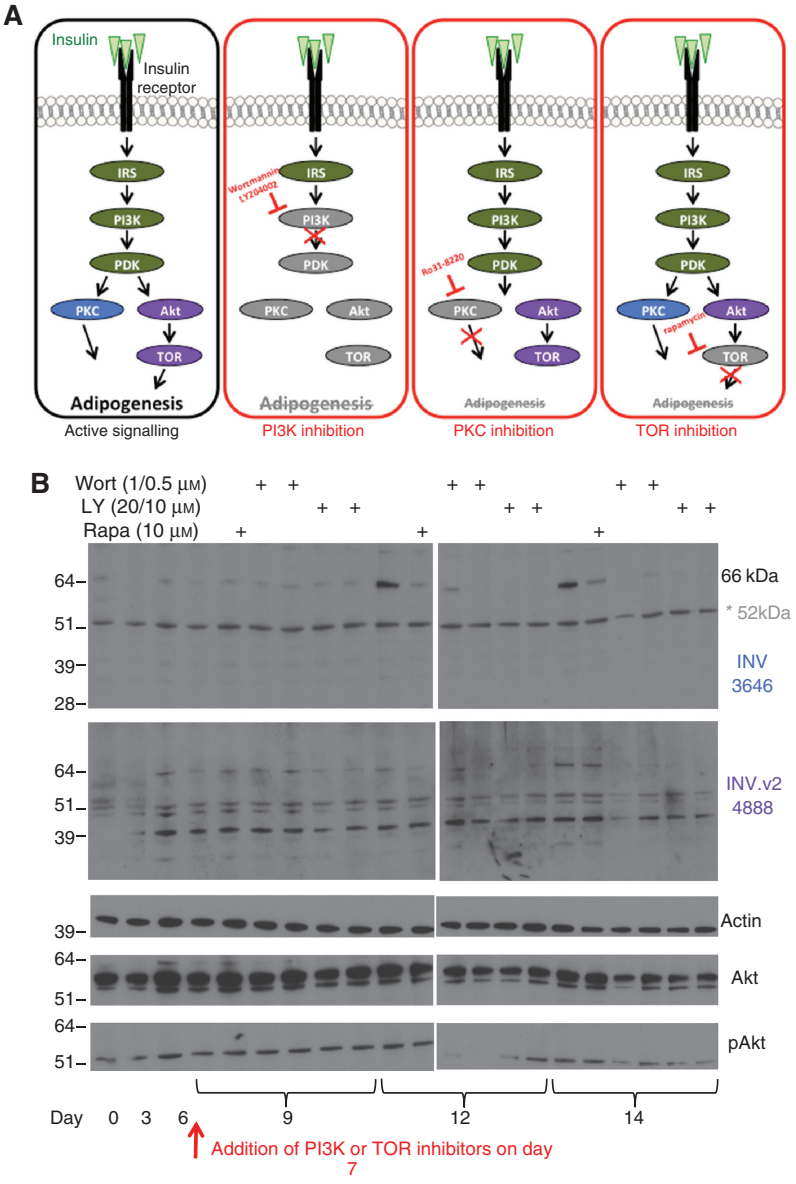

Figure 11: Effect of PI3K and TOR inhibitors during SGBS adipogenesis.
(A) A simplified schematic of the insulin/TOR pathway with key components such as insulin, insulin receptor, IRS (Insulin Receptor Substrate), PI3K, PDK, PKC, Akt, TOR kinase depicted. Wortmannin and LY294002 inhibit PI3K, while rapamycin is an inhibitor of TOR kinase. Inhibitors were added to SGBS cells on day 7 following induction of adipogenesis. (B) Immunoblotting of SGBS extracts using 3646 and 4888 invadolysin antibodies. The increase in the 66 kDa form of invadolysin (detected by both 3646 and 4888 antibodies) was diminished when adipogenesis was inhibited by PI3K inhibition, but less so by the inhibition of TOR kinase. *The 52 kDa form that remained constant during adipogenesis is detected by the secondary antibody alone and therefore unrelated to invadolysin. These results suggest that the level of INV.v2 might be regulated downstream of PI3K and upstream of TOR. The levels of pAkt decreased on days 12 and 14 upon addition of Wortmannin and LY294002, demonstrating inhibition of PI3K. The level of pAkt remained constant upon addition of Rapamycin (TOR inhibitor) as TOR is downstream of PI3K and Akt in the insulin signaling pathway.

the level of Lsd2, a protein that normally facilitates lipid storage. The localization of invadolysin to LDs during *de novo* formation of LDs is Protein Kinase C dependent. The N-terminus of invadolysin can be phosphorylated by PKC *in vitro*, suggesting that invadolysin may be phosphorylated *in vivo*. PKC is therefore a candidate for regulating the localization of invadolysin. Interestingly, invadolysin appears to localize differentially during distinct stages of 3T3-L1 adipogenesis, localizing to LDs during the early-mid stages of differentiation, but then appearing more homogeneously dispersed in later stage adipocytes. The level of invadolysin was significantly increased in both murine

3T3-L1 and human SGBS *in vitro* adipogenesis models. The increase in invadolysin was prevented when adipogenesis was blocked by PKC or PI3K inhibitors in 3T3-L1 cells, and PI3K inhibition in SGBS cells.

Invadolysin and insulin signaling

Examination of *D. invadolysin* mutants demonstrated that invadolysin plays a role in insulin signaling. The size of *invadolysin* mutant larvae is smaller than that of wild type larvae at the same stage. This is a common phenotype of *Drosophila* mutants in the insulin signaling pathway, which is known to play a crucial role in growth and metabolism (Garofalo, 2002; McHugh et al., 2004). We have previously demonstrated that the triglyceride:protein ratio was significantly reduced in *invadolysin* mutants compared to wild type animals (Cobbe et al., 2009). We have here shown that the glycogen:protein ratio is also decreased while autophagy is increased in *invadolysin* mutants. Our results confirmed that the level of active (phosphorylated) forms of pAkt and the downstream S6K and 4E-BP effectors of the insulin/TOR pathway were all decreased in *invadolysin* mutant larvae. These observations suggest that invadolysin may positively regulate the insulin signaling pathway, as insulin signaling positively affects fatty acid and glycogen synthesis, and negatively affects autophagy via TOR (Halse et al., 2001; Jung et al., 2010; Wong and Sul, 2010).

Insulin signaling has been implicated in the control of lipid metabolism in flies and mice. Both *S6K* and *4E-BP* mutant mice are lean and resistant to diet-induced obesity (Tsukiyama-Kohara et al., 2001; Um et al., 2004). *4E-BP* mutant flies show increased sensitivity to nutrient deprivation, leading to abnormal fat loss (Teleman et al., 2005). Akt promotes the transcription of genes involved in lipid biosynthesis and storage pathways (Eberlé et al., 2004; Vereshchagina and Wilson, 2006). Activation of Akt in *Drosophila* nurse cells results in the accumulation of Lsd2 (a homologue of perilipin) (Vereshchagina and Wilson, 2006). A decrease of pAkt and Lsd2 were observed in *invadolysin* mutant larvae. Recently, we have performed a microarray analysis to identify genes with altered expression in *invadolysin* mutant larvae. This analysis revealed an increase of 4E-BP and decrease of Lsd1 (another PAT family protein in *Drosophila*). These data will be detailed in a subsequent manuscript.

Lsd2 mutants exhibit impaired lipid storage, thus mutant larvae appear less opaque with a decreased triglyceride content than wild type larvae (Teixeira et al., 2003). We also documented decreased triglyceride:protein in *invadolysin* mutant larvae (Cobbe et al., 2009), which might be a consequence of decreased Lsd2. *Drosophila* wild type larvae accumulate significantly higher triglyceride on a high sucrose diet (Musselman et al., 2011). The ability to accumulate higher triglyceride levels on a high sugar diet was impaired in *invadolysin* mutant larvae. In light of these data, we hypothesize that invadolysin plays a homeostatic role, possibly by positively regulating insulin signaling.

The localization of invadolysin to nascent LDs was dependent on PKC activity

Invadolysin is the first metalloprotease reported to localize to LDs. Studies have shown that proteins can be anchored to LDs via a GPI anchor or via a N-terminal hydrophobic sequence (Müller et al., 2008; Zehmer et al., 2008). In this study, we showed that targeting of invadolysin to LDs was dependent on PKC activity. Treatment with a general PKC inhibitor decreased the formation of LDs in cells and caused invadolysin aggregates to form in the cytosol. When the PKC inhibitor was removed, invadolysin relocalized to LDs, suggesting that PKC activity plays a crucial role in regulating invadolysin's localization in the cellular starvation/refeeding model.

The starvation/refeeding experiments suggested that invadolysin might be recruited to nascent LDs. Invadolysin may bind to LDs via a hydrophobic GPI anchor, as there is a GPI-addition consensus sequence near the C-terminus of invadolysin (Cobbe et al., 2009). However, in the presence of a PKC inhibitor, fewer LDs were formed in cells and invadolysin may be forced to remain cytosolic leading to the self-association of invadolysin hydrophobic tails to form intracellular aggregates.

The use of a PKC inhibitor suggested that invadolysin's relocalization may also be regulated by PKC phosphorylation. Removal of the PKC inhibitor presumably resulted in the reactivation of PKC, during which the relocalization of invadolysin to LDs was observed, possibly because invadolysin could again be phosphorylated by PKC. An *in vitro* PKC assay revealed that targeting to LDs might be mediated by phosphorylation of Thr 220 and/or Thr269 within the N-terminal half of invadolysin. Interestingly, it has also been shown that the recruitment of caveolin to LDs in high levels of oleic acid or cholesterol was dependent on Src and PKC activity (Le Lay et al., 2006; Blouin et al., 2008).

Invadolysin plays a role in *in vitro* adipogenesis

The levels and localization of LD binding proteins are dynamically regulated during adipocyte differentiation.

Expression of the LD binding proteins CGI-58 and ADRP increased during adipocyte differentiation. The mRNA of adipose triglyceride lipase (ATGL) increased at days 4 and 6, but declined at day 8 during adipogenesis (Yamaguchi et al., 2004; Zimmermann et al., 2004). After a 10 min treatment of adipocytes with long chain fatty acids, small LDs emerged, surrounded by TIP47 and S3-12 (Wolins et al., 2006). Over the next hour of treatment, TIP47 and S3-12 still surrounded these small LDs, whereas ADRP was concentrated on intermediate LDs and perilipin on large LDs. The formation of LDs in the early stages appears to be important for their further growth (Brasaemle et al., 2004). In the later stages of adipogenesis, several LDs grew in size to more than 10 μm in diameter while the number of LDs drastically decreased. This suggests that the growth of LDs during adipocyte differentiation may be achieved by the successive fusion of LDs to one another.

Invadolysin displays a differential localization pattern during *in vitro* adipogenesis. In the early stages of differentiation (days 2–4), numerous small LDs appeared with invadolysin 'rings'. However, invadolysin appeared to be dispersed in the cytosol in day 8 adipocytes, and only bound small rather than large LDs in mature adipocytes (day 14). Invadolysin might be recruited to LDs during LD biogenesis in the early stages of adipogenesis (as observed in the starvation/refeeding model). An association of invadolysin with LDs at early times might be important for the recruitment of other LD-associated proteins or for the maintenance of LDs. At later stages of adipogenesis (after day 6), a role for invadolysin might be substituted by other proteins.

Although invadolysin was not observed on large LDs in mature adipocytes, the invadolysin level increased significantly during both 3T3-L1 and SGBS adipogenesis. Inhibition of adipogenesis by addition of inhibitors to 3T3-L1 and SGBS cells diminished the increase in invadolysin. The level of TIP47 did not change following inhibition of PKC and PI3K in 3T3-L1 cells, and TIP47 has been reported to be functionally unnecessary for adipogenesis (Yamaguchi et al., 2004). Our results shows a strong correlation between an increase in invadolysin and adipogenesis. Whether invadolysin is essential for adipogenesis will be best addressed by genetic *invadolysin* knock-out models, either through the examination of conditional knock-outs in tissues of interest, or by the differentialtion of mouse embryonic fibroblasts (Tontonoz et al., 1994; Yamakawa et al., 2008).

The process of adipocyte differentiation is modulated by the activity of numerous transcription factors, resulting in turn from activation of signaling pathways (Rosen and MacDougald, 2006). Many adipocyte-specific genes, including perilipin, are regulated by PPARγ, an essential transcription factor for adipogenesis (Rosen and Spiegelman, 2000). The presence of perilipin in 3T3-L1 cells would imply that the transcription factor PPARγ has been activated (Arimura et al., 2004). We demonstrated that perilipin and invadolysin mRNA levels were dramatically increased at day 2 of adipogenesis (and even further at day 4). This result suggested that the increase of invadolysin might be brought about by PPARγ or a downstream transcription factor such as C/EBPα. In the presence of PKC and PI3K inhibitors, the level of PPARγ was decreased (Zhou et al., 2006; Yu et al., 2008). Inhibition of PPARγ or studies on *PPARγ* null animals may help to elucidate any links between PPARγ and invadolysin in adipogenesis (Barak et al., 1999; Rosen et al., 1999).

Overall, our work provides new insights into the localization and role of invadolysin. Levels of p-Akt, p-S6K, p-4E-BP, and Lsd2 were decreased in *invadolysin* mutant larvae. The localization of invadolysin to newly synthesized LDs was dependent on PKC activity. An increase of invadolysin was observed during adipogenesis and blocked in the presence of PKC or PI3K inhibitors. These results suggest that invadolysin might normally play a positive role in the insulin signaling pathway and subsequently regulate lipid homeostasis. All of these data imply that invadolysin is a strong candidate for positive regulation of adipocyte differentiation via insulin signaling.

Materials and methods

Antibodies and reagents

Antibodies used in this work were 3645/6 = INV P1-Ab (Cobbe et al., 2009), INV C-Ab1 (Cobbe et al., 2009), 4624 (INV.v1 downstream of signal sequence: SLGSSPPCRHHVPS), 4888 (INV.v2 N-terminal region: SGLLGLRPGPEPVAL), perilipin (Sigma-Aldrich), TIP-47 (Progen), Akt, phospho-Akt 505, phospho-p70 S6 kinase Thr 398, and phospho-4E-BP Thr37/46 (all Cell Signaling, Genosphere, Paris, France). The invadolysin peptide antibodies were generated by Genosphere. Lsd2 antibodies were generously provided by Dr. Ronald Kühnlein (Max Planck Institute, Munich) and Dr. Luis Teixeira (University of Cambridge). PKC inhibitors Ro31-8220, Cycloheximide, 3-isobutyl-l-methylxantin (IBMX), dexamethasone (DEX) and insulin were purchased from Sigma-Aldrich. PI-3 kinase (PI3K) was obtained from Cell Signaling.

Cell culture

Cells were cultured in a humidified incubator at 37°C with 5% CO_2. For HeLa (human cervical carcinoma) and A375 (human melanoma) cells, DMEM (Dulbecco's Modified Essential Medium, GIBCO) with

10% FBS was used. For 3T3-L1 cells (mouse embryonic fibroblasts), DMEM with 10% newborn calf serum (NCS) was used. For starvation and refeeding experiments, cells were starved in DMEM without serum for 24 h, and cells were refed with DMEM containing 10% FBS and 10 μM oleic acid (Sigma-Aldrich). In some experiments, inhibitors were added 1 h before supplementing the medium with 10% FBS and 10 μM oleic acid.

Adipocyte differentiation

3T3-L1 differentiation: Mouse embryonic 3T3-L1 cells were cultured in DMEM + 10% NCS until confluent. Two days after confluence, cells were stimulated with DMEM+10% FBS containing 100 μM IBMX (Sigma, I7018), 0.25 μM DEX (Sigma, D4902) and 1 μg/ml insulin (Sigma, I5500). A change of cellular morphology was observed over the next 48 h. After stimulation, the culture medium was replaced with fresh medium containing 1 μg/ml insulin every 48 h for 2 times. Afterwards, the culture medium was replaced with DMEM + 10% FBS medium. At day 8, cells were fully differentiated (Student et al., 1980).

SGBS differentiation: SGBS cells are a human preadipocyte cell line obtained from subcutaneous white adipose depot of a patient suffering form SGBS disease (Wabitsch et al., 2001). These cells can be stimulated to be differentiated into adipocytes. For adipogenesis of SGBS cells, previously established protocol by Posovsky et al. was used (Fischer-Posovszky et al., 2008). SGBS cells were cultured in DMEM/F12 (life technologies) medium supplemented with 10% fetal bovine serum and containing 33 μM biotin and 17 μM pantothenic acid. For initiating adipogenesis the cells were allowed to reach 90–95% confluency. On day 0, adipogenesis is initiated in a DMEM/F12 medium with 33 μM biotin and 17 μM pantothenic acid in absence of serum containing a cocktail of drugs (0.1 μM cortisol, 20 nM insulin, 250 nM dexamethasone, 500 μM IBMX and 2 μM rosiglitazone). On day 3, rosiglitazone was withdrawn from the differentiation medium and on day 7, IBMX and dexamethasone were removed. The cells were allowed to differentiate until day 14 under these conditions.

RT-PCR and qPCR

Total RNA from cultured cells or *Drosophila* larvae was extracted using the RNeasy® Mini Kit (Qiagen, 74104) according to manufacturer's instructions and as previously described (Cobbe et al., 2009). RT-PCR reactions were performed using Superscript III reverse transcriptase (Invitrogen) in 20 μl reactions according to the manufacturer's instructions. PCR reactions were performed with primers designed to span exon boundaries. qPCR was performed using the LightCycler® 480 System and the LighterCycler® 480 probes Master kit (Roche). Primers and probes used in qPCR reactions were designed by Universal Probe Library Assay Design Center by entering the sequence ID from Ensembl.

In vitro kinase assay

The *in vitro* phosphorylation assay of invadolysin was performed at 30°C in a 20 μl reaction. The reaction contained 1× kinase buffer (25 mM Tris-HCl pH7.5, 5 mM β-glycerophosphate, 2 mM DTT, 0.1 mM Na_3VO_4, 10 mM $MgCl_2$), 200 μM cold ATP (Cell Signaling, 9804), 1 μg of purified protein kinase C (Calbiochem, 539494), 0.1–1 μg of substrate, and 0.2 μl of γ-32P-ATP (Perkin Ekmer, 250UC, NEG 502Z). After a 30 min incubation, 10 μl of 3× SDS-PAGE sample buffer [6% SDS, 150 mM upper buffer Tris (pH6.8), 30% Glycerol, 0.03% Bromophenol blue, 6 mM EDTA] was added to the reaction mixture and the mixture was boiled for 10 min. The samples were then resolved by 4–12% SDS-PAGE. After electrophoresis, the gel was transferred to Whatman blotting paper and dried for 2 h in a heated gel dryer. The dried gel was exposed to Lumi-Film Chemiuminescent detection film.

Preparation of protein extracts

From cultured cells: Medium was removed and the cells were rinsed with PBS. 200 μl of RIPA lysis buffer with protease inhibitors (Roche Protease Inhibitor Cocktail Tablets) were added into each well of a 6-well plate (35 mm culture dish), the cells were scraped and the resulting cell lysate was then transferred to a 1.5 ml Eppendorf tube. The lysate was mixed with 100 μl of 3× SDS-PAGE sample buffer confaining DTT and the mixture was sonicated 5 times (2 s sonication with 5 s rest intervals), and subsequently boiled for 10 min. To remove the debris, the tube was centrifuged at 10 000 *g* for 2 min at 4°C, and the supernatant was collected and stored at –20°C until required.

From larvae: 3-day-old adult flies of the appropriate genotype were transferred into a cage containing an apple juice agar plate with fresh yeast paste and allowed to lay eggs for 24 h. Adult flies were then removed and the plate with eggs was placed in a 25°C incubator. 72 h after hatching from eggs, approximately 8–10 larvae were transferred to a vial containing fresh fly food supplemented with yeast paste. 24 h later, larvae of the appropriate genotype were collected (5 wild type larvae and 15 mutant larvae), rinsed with PBS and transferred to 1.5 ml Eppendorf tubes with 100 μl EBR lysis buffer (Ephrussi-Beadle Ringer's: 130 mM NaCl, 4.7 mM KCl, 1.9 mM $CaCl_2$, 10 mM HEPES, pH6.9) with protease and phosphatase inhibitors. The larvae were homogenized on ice with a hand pestle. Another 200 μl of ice cold EBR lysis buffer was added to the tubes and mixed gently by pipetting. The homogenate was mixed with 150 μl of 3× SDS-PAGE sample buffer and 10 μl of 1M DTT. The mixture was then sonicated for 2 s with 5 s rest intervals for 5 times and subsequently boiled for 10 min. To remove the debris, the tube was centrifuged at 10 000 *g* for 2 min at 4°C, and the supernatant was collected and stored at –20°C.

From larval fat body: 96-h-old larvae of the appropriate genotype were collected and rinsed in a glass dish pre-filled with cold PBS and protease inhibitors. The larvae were dissected by the 'pull and drag' method with two pairs of forceps. This method exposes all internal organs to the PBS. The fat bodies were transferred to an Eppendorf tube containing 100 μl EBR lysis buffer (10 fat bodies from wild type and 40 fat bodies from *invadolysin* mutant were collected). The fat bodies were then homogenized on ice with a hand pestle. Another 200 μl of cold EBR lysis buffer was added to the tubes and mixed gently by pipetting. The homogenate was mixed with 150 μl of 3× SDS-PAGE sample buffer and 10 μl of 1M DTT. The mixture was then sonicated for 2 s with 5 s rest intervals for 5 times and subsequently boiled for 10 min. To remove the debris, the tube was centrifuged at 10 000 *g* for 2 min at 4°C, and the supernatant was collected and stored at –20°C.

SDS-PAGE and immunoblotting

Cell lysates were subjected to SDS-PAGE and immunoblotted as previously reported (Cobbe et al., 2009). Nitrocellulose membranes were probed with desired antibodies. Primary antibody detection was performed using an appropriate horseradish peroxidase-conjugated IgG, and the immune-signal was detected by ECL (GE Healthcare) with Lumi-Film Chemiluminescent detection film (Roche).

Immunofluorescence

The procedures used were previously described (Cobbe et al., 2009). Cultured cells were seeded overnight onto round cover slips. Cover slips were removed from the culture dish and fixed for 3 min with 4% formaldehyde and cells permeabilised with PBS containing 0.1% TX-100 for 3 min. After washing twice with PBST (PBS containing 0.05% TX-100), cells were blocked with PBS + 3% BSA at room temperature for 30 min. After washing twice in PBST, cells were incubated with primary antibody for 1 h at room temperature. After washing 3 times in PBST, cells were incubated with the secondary antibody at room temperature for 45 min. After washing 3 times in PBST, the cover slips were mounted on glass slides with a Mowiol solution. Cells were visualized with an Olympus AX-70 Provis epifluorescence microscope equipped with a Hamamatsu Orca II CCD camera and SmartCapture3 software.

References

Accioly, M.T., Pacheco, P., Maya-Monteiro, C.M., Carrossini, N., Robbs, B.K., Oliveira, S.S., Kaufmann, C., Morgado-Diaz, J.A., Bozza, P.T., and Viola, J.P. (2008). Lipid bodies are reservoirs of cyclooxygenase-2 and sites of prostaglandin-E2 synthesis in colon cancer cells. Cancer Res. *68*, 1732–1740.

Akimoto, N., Sato, T., Iwata, C., Koshizuka, M., Shibata, F., Nagai, A., Sumida, M., and Ito, A. (2005). Expression of perilipin A on the surface of lipid droplets increases along with the differentiation of hamster sebocytes *in vivo* and *in vitro*. J. Invest. Dermatol. *124*, 1127–1133.

Andersson, L., Bostrom, P., Ericson, J., Rutberg, M., Magnusson, B., Marchesan, D., Ruiz, M., Asp, L., Huang, P., Frohman, M.A., et al. (2006). PLD1 and ERK2 regulate cytosolic lipid droplet formation. J. Cell Sci. *119*, 2246–2257.

Arimura, N., Horiba, T., Imagawa, M., Shimizu, M., and Sato, R. (2004). The peroxisome proliferator-activated receptor g regulates expression of the perilipin gene in adipocytes. J. Biol. Chem. *279*, 10070–10076.

Aubin, D., Gagnon, A., and Sorisky, A. (2005). Phosphoinositide 3-kinase is required for human adipocyte differentiation in culture. Int. J. Obes. (Lond.) *29*, 1006–1009.

Barak, Y., Nelson, M.C., Ong, E.S., Jones, Y.Z., Ruiz-Lozano, P., Chien, K.R., Koder, A., and Evans, R.M. (1999). PPARg is required for placental, cardiac, and adipose tissue development. Mol. Cell *4*, 585–595.

Bartz, R., Zehmer, J.K., Zhu, M., Chen, Y., Serrero, G., Zhao, Y., and Liu, P. (2007). Dynamic activity of lipid droplets: protein phosphorylation and GTP-mediated protein translocation. J. Proteome. Res. *6*, 3256–3265.

Blom, N., Gammeltoft, S., and Brunak, S. (1999). Sequence and structure-based prediction of eukaryotic protein phosphorylation sites. J. Mol. Biol. *294*, 1351–1362.

Blom, N., Sicheritz-Pontén, T., Gupta, R., Gammeltoft, S., and Brunak, S. (2004). Prediction of post-translational glycosylation and phosphorylation of proteins from the amino acid sequence. Proteomics *4*, 1633–1649.

Blouin, C.M., Le Lay, S., Lasnier, F., Dugail, I., and Hajduch, E. (2008). Regulated association of caveolins to lipid droplets during differentiation of 3T3-L1 adipocytes. Biochem. Biophys. Res. Commun. *376*, 331–335.

Brasaemle, D.L., Dolios, G., Shapiro, L., and Wang, R. (2004). Proteomic analysis of proteins associated with lipid droplets of basal and lipolytically stimulated 3T3-L1 adipocytes. J. Biol. Chem. *279*, 46835–46842.

Cermelli, S., Guo, Y., Gross, S.P., and Welte, M.A. (2006). The lipid-droplet proteome reveals that droplets are a protein-storage depot. Curr. Biol. *16*, 1783–1795.

Chen, J.S., Greenberg, A.S., and Wang, S.M. (2002). Oleic acid-induced PKC isozyme translocation in RAW 264.7 macrophages. J. Cell Biochem. *86*, 784–791.

Chikte, S., Panchal, N., and Warnes, G. (2014). Use of LysoTracker dyes: a flow cytometric study of autophagy. Cytometry A *85*, 169–178.

Cobbe, N., Marshall, K.M., Gururaja Rao, S., Chang, C.W., Di Cara, F., Duca, E., Vass, S., Kassan, A., and Heck, M.M. (2009). The conserved metalloprotease invadolysin localizes to the surface of lipid droplets. J. Cell Sci. *122*, 3414–3423.

Di Cara, F., Duca, E., Dunbar, D.R., Cagney, G., and Heck, M.M. (2013). Invadolysin, a conserved lipid-droplet-associated metalloproteinase, is required for mitochondrial function in *Drosophila*. J. Cell Sci. *126*, 4769–4781.

Eberlé, D., Hegarty, B., Bossard, P., Ferré, P., and Foufelle, F. (2004). SREBP transcription factors: master regulators of lipid homeostasis. Biochimie *86*, 839–848.

El-Chaâr, D., Gagnon, A., and Sorisky, A. (2004). Inhibition of insulin signaling and adipogenesis by rapamycin: effect on phosphorylation of p70 S6 kinase vs eIF4E-BP1. Int. J. Obes. Relat. Metab. Disord. *28*, 191–198.

Farmer, S.R. (2006). Transcriptional control of adipocyte formation. Cell Metab. *4*, 263–273.

Fingar, D.C. and Blenis, J. (2004). Target of rapamycin (TOR): an integrator of nutrient and growth factor signals and coordinator of cell growth and cell cycle progression. Oncogene *23*, 3151–3171.

Fischer-Posovszky, P., Newell, F.S., Wabitsch, M., and Tornqvist, H.E. (2008). Human SGBS cells-a unique tool for studies of human fat cell biology. Obes. Facts *1*, 184–189.

Fleming, I., MacKenzie, S.J., Vernon, R.G., Anderson, N.G., Houslay, M.D., and Kilgour, E. (1998). Protein kinase C isoforms play differential roles in the regulation of adipocyte differentiation. Biochem. J. *333*, 719–727.

Garofalo, R.S. (2002). Genetic analysis of insulin signaling in *Drosophila*. Trends Endocrinol. Metab. *13*, 156–162.

Goldberg, A.A., Bourque, S.D., Kyryakov, P., Boukh-Viner, T., Gregg, C., Beach, A., Burstein, M.T., Machkalyan, G., Richard, V., Rampersad, S., et al. (2009). A novel function of lipid droplets in regulating longevity. Biochem. Soc. Trans. *37*, 1050–1055.

Gomis-Ruth, F.X. (2003). Structural aspects of the metzincin clan of metalloendopeptidases. Mol. Biotechnol. *24*, 157–202.

Green, H. and Kehinde, O. (1976). Spontaneous heritable changes leading to increased adipose conversion in 3T3 cells. Cell *7*, 105–113.

Halse, R., Bonavaud, S.M., Armstrong, J.L., McCormack, J.G., and Yeaman, S.J. (2001). Control of glycogen synthesis by glucose, glycogen, and insulin in cultured human muscle cells. Diabetes *50*, 720–726.

Holm, C. (2003). Molecular mechanisms regulating hormone-sensitive lipase and lipolysis. Biochem. Soc. Trans. *31*, 1120–1124.

Imamura, M., Inoguchi, T., Ikuyama, S., Taniguchi, S., Kobayashi, K., Nakashima, N., and Nawata, H. (2002). ADRP stimulates lipid accumulation and lipid droplet formation in murine fibroblasts. Am. J. Physiol. Endocrinol. Metab. *283*, E775–783.

Inoki, K., Li, Y., Zhu, T., Wu, J., and Guan, K.L. (2002). TSC2 is phosphorylated and inhibited by Akt and suppresses mTOR signalling. Nat. Cell Biol. *4*, 648–657.

Jung, C.H., Ro, S.H., Cao, J., Otto, N.M., and Kim, D.H. (2010). mTOR regulation of autophagy. FEBS Lett. *584*, 1287–1295.

Kim, J.E. and Chen, J. (2004). regulation of peroxisome proliferator-activated receptor- g activity by mammalian target of rapamycin and amino acids in adipogenesis. Diabetes *53*, 2748–2756.

Lawrence, J.C., Lin, T.A., McMahon, L.P., and Choi, K.M. (2004). Modulation of the protein kinase activity of mTOR. Curr. Top Microbiol. Immunol. *279*, 199–213.

Le Lay, S., Hajduch, E., Lindsay, M.R., Le Liẽpvre, X., Thiele, C., Ferré, P., Parton, R.G., Kurzchalia, T., Simons, K., and Dugail, I. (2006). Cholesterol-induced caveolin targeting to lipid droplets in adipocytes: a role for caveolar endocytosis. Traffic *7*, 549–561.

Li, Z., Thiel, K., Thul, P.J., Beller, M., Kühnlein, R.P., and Welte, M.A. (2012). Lipid droplets control the maternal histone supply of *Drosophila* embryos. Curr. Biol. *22*, 2104–2113.

Manning, B.D., Tee, A.R., Logsdon, M.N., Blenis, J., and Cantley, L.C. (2002). Identification of the tuberous sclerosis complex-2 tumor suppressor gene product tuberin as a target of the phosphoinositide 3-kinase/akt pathway. Mol. Cell *10*, 151–162.

McHugh, B., Krause, S.A., Yu, B., Deans, A.M., Heasman, S., McLaughlin, P., and Heck, M.M. (2004). Invadolysin: a novel, conserved metalloprotease links mitotic structural rearrangements with cell migration. J. Cell Biol. *167*, 673–686.

Miura, S., Gan, J.W., Brzostowski, J., Parisi, M.J., Schultz, C.J., Londos, C., Oliver, B., and Kimmel, A.R. (2002). Functional conservation for lipid storage droplet association among Perilipin, ADRP, and TIP47 (PAT)-related proteins in mammals, *Drosophila*, and *Dictyostelium*. J. Biol. Chem. *277*, 32253–32257.

Müller, G., Over, S., Wied, S., and Frick, W. (2008). Association of (c) AMP-degrading glycosylphosphatidylinositol-anchored proteins with lipid droplets is induced by palmitate, H_2O_2 and the sulfonylurea drug, glimepiride, in rat adipocytes. Biochemistry *47*, 1274–1287.

Munafó, D.B. and Colombo, M.I. (2001). A novel assay to study autophagy: regulation of autophagosome vacuole size by amino acid deprivation. J. Cell Sci. *114*, 3619–3629.

Musselman, L.P., Fink, J.L., Narzinski, K., Ramachandran, P.V., Hathiramani, S.S., Cagan, R.L., and Baranski, T.J. (2011). A high-sugar diet produces obesity and insulin resistance in wild-type *Drosophila*. Dis. Models Mech. *4*, 842–849.

Naslavsky, N., Rahajeng, J., Rapaport, D., Horowitz, M., and Caplan, S. (2007). EHD1 regulates cholesterol homeostasis and lipid droplet storage. Biochem. Biophys. Res. Commun. *357*, 792–799.

Norman, B.H., Shih, C., Toth, J.E., Ray, J.E., Dodge, J.A., Johnson, D.W., Rutherford, P.G., Schultz, R.M., Worzalla, J.F., and Vlahos, C.J. (1996). Studies on the mechanism of phosphatidylinositol 3-kinase inhibition by wortmannin and related analogs. J. Med. Chem. *39*, 1106–1111.

Oshiro, N., Yoshino, K., Hidayat, S., Tokunaga, C., Hara, K., Eguchi, S., Avruch, J., and Yonezawa, K. (2004). Dissociation of raptor from mTOR is a mechanism of rapamycin-induced inhibition of mTOR function. Genes. Cells *9*, 359–366.

Ozeki, S., Cheng, J., Tauchi-Sato, K., Hatano, N., Taniguchi, H., and Fujimoto, T. (2005). Rab18 localizes to lipid droplets and induces their close apposition to the endoplasmic reticulum-derived membrane. J. Cell Sci. *118*, 2601–2611.

Potter, C.J., Pedraza, L.G., and Xu, T. (2002). Akt regulates growth by directly phosphorylating Tsc2. Nat. Cell Biol. *4*, 658–665.

Prusty, D., Park, B.H., Davis, K.E., and Farmer, S.R. (2002). Activation of MEK/ERK signaling promotes adipogenesis by enhancing peroxisome proliferator-activated receptor gamma (PPARg) and C/EBPa gene expression during the differentiation of 3T3-L1 preadipocytes. J. Biol. Chem. *277*, 46226–46232.

Rao, S.G., Janiszewski, M.M., Duca, E., Nelson, B., Abhinav, K., Panagakou, I., Vass, S., and Heck, M.M. (2015). Invadolysin acts genetically via the SAGA complex to modulate chromosome structure. Nucleic Acids Res. *43*, 3546–3562.

Rawlings, N.D. and Barrett, A.J. (1999). MEROPS: the peptidase database. Nucleic Acids Res. *27*, 325–331.

Rosen, E.D. and MacDougald, O.A. (2006). Adipocyte differentiation from the inside out. Nat. Rev. Mol. Cell Biol. *7*, 885–896.

Rosen, E.D. and Spiegelman, B.M. (2000). Peroxisome proliferator-activated receptor g ligands and atherosclerosis: ending the heartache. J. Clin. Invest. *106*, 629–631.

Rosen, E.D., Sarraf, P., Troy, A.E., Bradwin, G., Moore, K., Milstone, D.S., Spiegelman, B.M., and Mortensen, R.M. (1999). PPARg is required for the differentiation of adipose tissue *in vivo* and *in vitro*. Mol. Cell *4*, 611–617.

Sakaue, H., Ogawa, W., Matsumoto, M., Kuroda, S., Takata, M., Sugimoto, T., Spiegelman, B.M., and Kasuga, M. (1998). Post-transcriptional control of adipocyte differentiation through activation of phosphoinositide 3-kinase. J. Biol. Chem. *273*, 28945–28952.

Scherzer, C.R., Jensen, R.V., Gullans, S.R., and Feany, M.B. (2003). Gene expression changes presage neurodegeneration in a *Drosophila* model of Parkinson's disease. Hum. Mol. Genet. *12*, 2457–2466.

Smirnova, E., Goldberg, E.B., Makarova, K.S., Lin, L., Brown, W.J., and Jackson, C.L. (2006). ATGL has a key role in lipid droplet/adiposome degradation in mammalian cells. EMBO Rep. *7*, 106–113.

Student, A.K., Hsu, R.Y., and Lane, M.D. (1980). Induction of fatty acid synthetase synthesis in differentiating 3T3-L1 preadipocytes. J. Biol. Chem. *255*, 4745–4750.

Taniguchi, C.M., Emanuelli, B., and Kahn, C.R. (2006). Critical nodes in signalling pathways: insights into insulin action. Nat. Rev. Mol. Cell Biol. *7*, 85–96.

Teixeira, L., Rabouille, C., Rørth, P., Ephrussi, A., and Vanzo, N.F. (2003). *Drosophila* Perilipin/ADRP homologue Lsd2 regulates lipid metabolism. Mech. Dev. *120*, 1071–1081.

Teleman, A.A., Chen, Y.W., and Cohen, S.M. (2005). 4E-BP functions as a metabolic brake used under stress conditions but not during normal growth. Genes. Dev. *19*, 1844–1848.

Tontonoz, P., Hu, E., and Spiegelman, B.M. (1994). Stimulation of adipogenesis in fibroblasts by PPARg 2, a lipid-activated transcription factor. Cell *79*, 1147–1156.

Tseng, Y.H., Kriauciunas, K.M., Kokkotou, E., and Kahn, C.R. (2004). Differential roles of insulin receptor substrates in brown adipocyte differentiation. Mol. Cell Biol. *24*, 1918–1929.

Tsukiyama-Kohara, K., Poulin, F., Kohara, M., DeMaria, C.T., Cheng, A., Wu, Z., Gingras, A.C., Katsume, A., Elchebly, M., Spiegelman, B.M., et al. (2001). Adipose tissue reduction in mice lacking the translational inhibitor 4E-BP1. Nat. Med. *7*, 1128–1132.

Turro, S., Ingelmo-Torres, M., Estanyol, J.M., Tebar, F., Fernandez, M.A., Albor, C.V., Gaus, K., Grewal, T., Enrich, C., and Pol, A. (2006). Identification and characterization of associated with lipid droplet protein 1: a novel membrane-associated protein that resides on hepatic lipid droplets. Traffic *7*, 1254–1269.

Um, S.H., Frigerio, F., Watanabe, M., Picard, F., Joaquin, M., Sticker, M., Fumagalli, S., Allegrini, P.R., Kozma, S.C., Auwerx, J., et al. (2004). Absence of S6K1 protects against age- and diet-induced obesity while enhancing insulin sensitivity. Nature *431*, 200–205.

Vass, S. and Heck, M.M. (2013). Perturbation of invadolysin disrupts cell migration in zebrafish (*Danio rerio*). Exp. Cell Res. *319*, 1198–1212.

Vereshchagina, N. and Wilson, C. (2006). Cytoplasmic activated protein kinase Akt regulates lipid-droplet accumulation in *Drosophila* nurse cells. Development *133*, 4731–4735.

Vlahos, C.J., Matter, W.F., Hui, K.Y., and Brown, R.F. (1994). A specific inhibitor of phosphatidylinositol 3-kinase, 2-(4-morpholinyl)-8-phenyl-4H-1-benzopyran-4-one (LY294002). J. Biol. Chem. *269*, 5241–5248.

Wabitsch, M., Brenner, R.E., Melzner, I., Braun, M., Möller, P., Heinze, E., Debatin, K.M., and Hauner, H. (2001). Characterization of a human preadipocyte cell strain with high capacity for adipose differentiation. Int. J. Obes. Relat. Metab. Disord. *25*, 8–15.

Walther, T.C. and Farese, R.V. (2012). Lipid droplets and cellular lipid metabolism. Annu. Rev. Biochem. *81*, 687–714.

Wang, Z., Wilson, W.A., Fujino, M.A., and Roach, P.J. (2001). Antagonistic controls of autophagy and glycogen accumulation by Snf1p, the yeast homolog of AMP-activated protein kinase, and the cyclin-dependent kinase Pho85p. Mol. Cell Biol. *21*, 5742–5752.

Welte, M.A. (2015). Expanding roles for lipid droplets. Curr. Biol. *25*, R470–R481.

Wolins, N.E., Quaynor, B.K., Skinner, J.R., Tzekov, A., Croce, M.A., Gropler, M.C., Varma, V., Yao-Borengasser, A., Rasouli, N., Kern, P.A., et al. (2006). OXPAT/PAT-1 is a PPAR-induced lipid droplet protein that promotes fatty acid utilization. Diabetes *55*, 3418–3428.

Wong, R.H. and Sul, H.S. (2010). Insulin signaling in fatty acid and fat synthesis: a transcriptional perspective. Curr. Opin. Pharmacol. *10*, 684–691.

Xuan, J.Y., Hughes-Benzie, R.M., and MacKenzie, A.E. (1999). A small interstitial deletion in the GPC3 gene causes Simpson-Golabi-Behmel syndrome in a Dutch-Canadian family. J. Med. Genet. *36*, 57–58.

Xue, Y., Ren, J., Gao, X., Jin, C., Wen, L., and Yao, X. (2008). GPS 2.0, a tool to predict kinase-specific phosphorylation sites in hierarchy. Mol. Cell Proteomics *7*, 1598–1608.

Yamaguchi, T., Omatsu, N., Matsushita, S., and Osumi, T. (2004). CGI-58 interacts with perilipin and is localized to lipid droplets. Possible involvement of CGI-58 mislocalization in Chanarin-Dorfman syndrome. J. Biol. Chem. *279*, 30490–30497.

Yamakawa, T., Whitson, R.H., Li, S.L., and Itakura, K. (2008). Modulator recognition factor-2 is required for adipogenesis in mouse embryo fibroblasts and 3T3-L1 cells. Mol. Endocrinol. *22*, 441–453.

Yang, Q., Inoki, K., Kim, E., and Guan, K.L. (2006). TSC1/TSC2 and Rheb have different effects on TORC1 and TORC2 activity. Proc. Natl. Acad. Sci. USA *103*, 6811–6816.

Yu, W., Chen, Z., Zhang, J., Zhang, L., Ke, H., Huang, L., Peng, Y., Zhang, X., Li, S., Lahn, B.T., et al. (2008). Critical role of phosphoinositide 3-kinase cascade in adipogenesis of human mesenchymal stem cells. Mol. Cell Biochem. *310*, 11–18.

Zehmer, J.K., Bartz, R., Liu, P., and Anderson, R.G. (2008). Identification of a novel N-terminal hydrophobic sequence that targets proteins to lipid droplets. J. Cell Sci. *121*, 1852–1860.

Zhou, Y., Wang, D., Li, F., Shi, J., and Song, J. (2006). Different roles of protein kinase C-bI and -d in the regulation of adipocyte differentiation. Int J Biochem Cell Biol. *38*, 2151–2163.

Zimmermann, R., Strauss, J.G., Haemmerle, G., Schoiswohl, G., Birner-Gruenberger, R., Riederer, M., Lass, A., Neuberger, G., Eisenhaber, F., Hermetter, A., et al. (2004). Fat mobilization in adipose tissue is promoted by adipose triglyceride lipase. Science *306*, 1383–1386.

Zirin, J., Nieuwenhuis, J., and Perrimon, N. (2013). Role of autophagy in glycogen breakdown and its relevance to chloroquine myopathy. PLoS Biol. *11*, e1001708.

Supplemental Material: The online version of this article (DOI: 10.1515/hsz-2016-0226) offers supplementary material, available to authorized users.